Molecular dynamics simulation of adhesion at the asphalt-aggregate interface: a review

Yujie Tang[a], Zhen Fu[a, *], Guido Raos[b], Feng Ma[c], Peng Zhao[a, *], Yingjie Hou[c]

[a] School of Materials Science and Engineering, Chang'an University, Xi'an, Shaanxi, 710064, China

[b] Department of Chemistry, Materials and Chemical Engineering "G. Natta", Politecnico di Milano, I-20131 Milano, Italy

[c] School of Highway, Chang'an University, Xi'an, Shaanxi, 710064, China

Abstract

Interfacial adhesion at the molecular level is a complex process, where the key players (asphalt, aggregates, water, and air) are in a dynamic state of structural equilibrium, varying rapidly under different environments and conditions. Most experimental tests, while capable of providing crucial information for practical application, are ill-suited to characterize molecular-level behavior of these materials. Molecular dynamics (MD) simulation provides a unique perspective into the dynamic world of asphalt-aggregate interfaces. It allows to directly monitor physiochemical processes that depend on the structural distribution, molecular composition, external load, and atomic mobility. Over the past decade, MD simulation has provided important insights into the dynamical processes that control interactions at asphalt-aggregate

* Corresponding author: Zhen Fu and Peng Zhao. E-mail address: yujietang2022@chd.edu.cn (Y.J. Tang); zhenfu@chd.edu.cn (Z. Fu); guido.raos@polimi.it (G. Raos); mafeng@chd.edu.cn (F. Ma); 963043279@qq.com (P. Zhao); yingjiehou@chd.edu.cn (Y.J. Hou)

interfaces, including adhesion, cohesion, diffusion, aggregation, binding, distribution, and aging, among others. This review covers both theoretical models and practical methods which provide a reliable and computationally efficient tool to incorporate certain microscopic details and correlations. This review also provides a comprehensive account of applications of MD to asphalt-aggregate interfaces and the advances it has enables in adhesion property of asphalt, with an emphasis on insights into model construction and performance of interfaces evaluation methods.

Keywords: molecular dynamics simulation, adhesion, asphalt, aggregate, interface

1. Introduction

Asphalt is a complex heterogeneous mixture, with the aggregate and the binder as the main phases. The interfacial adhesion between asphalt binder and aggregate is important in constructing a well-behaved, sustainable, and long-lived asphalt pavement[1, 2]. It does not only depend on the nature of composition materials like asphalt, modifier, aggregates, and fillers, but also on external factors like light, oxygen, heat, and water. Once interfacial adhesion is reduced, the overall performance of asphalt mixture is significantly damaged. The insufficient adhesion between asphalt and aggregate can lead to asphalt peeling off from the surface of the aggregate when subjected to driving loads or temperature and humidity stress, leading to peeling and cracking of the asphalt pavement. Understanding the adhesion mechanisms between asphalt and aggregates is vital for optimizing the performance of asphalt pavements. Previous studies have proposed seven prominent theories to elucidate the complex

41 interplay of factors contributing to adhesion at the asphalt-aggregate interface. These
42 theories included: (i) Mechanics theory, (ii) Chemical reaction theory, (iii) Weak
43 boundary theory, (iv) Molecular orientation theory, (v) Electrostatic theory, (vi) Surface
44 structure theory, and (vii) Surface free energy theory, which described the
45 thermodynamic aspects of adhesion by considering energy exchange during the
46 formation of a new interface when the asphalt binder wets the aggregate surface[3].

47 Despite numerous theories have been proposed to elucidate the adhesion, none of
48 them can really explain all the data that are being produced at an increasing rate by
49 modern experimental methods. Technological advancements have enabled researchers
50 to employ a range of direct and indirect observation and characterization techniques to
51 delve into interfacial adhesion. Techniques such as scanning electron microscopy (SEM)
52 offers insights into surface morphology and adhesion characteristics of both aggregates
53 and asphalt[4-6]; X-ray computed tomography (X-ray CT) allows the analysis of void
54 distributions and aggregate structures within asphalt mixtures[7]; Atomic force
55 microscopy (AFM) facilitates exploration of the nanoscale morphology of asphalt and
56 aggregates[8, 9]. Additionally, several other experimental methods such as fluorescence
57 microscope, Ultra depth of field 3D scanning technology, nanoindentation have
58 contributed to this endeavor. However, despite notable progress, challenges persist in
59 achieving a comprehensive microscopic understanding of asphalt-aggregate adhesion
60 mechanisms solely through experimental means.

61 In recent years, the exponential growth of data generated by MD has sparked a

surge in interest regarding the development and utilization of this computational technique[10-13]. MD has found wide-ranging applications in chemistry, biology, energy, and materials research. The application of MD simulation has proven successful in various fields, e.g., ionic liquid electrolytes for battery[14], crystal nucleation in liquids[15], proteins, membranes, enzymes, and drugs discovery in biophysics[16-18], and petroleum and natural gas industries[19]. In cases where microscopic mechanisms failed to directly observed or explained through macroscopic experiments, especially at the molecular or atomic levels, MD, along with related methods such as density functional theory (DFT), Monte Carlo (MC) simulations, and quantum mechanics (QM), offered indispensable assistance. Compared with other macroscale characterization methods, MD simulation presented several noteworthy advantages: (i) Computational simulation could save time, economic, and labor costs required for experiments; (ii) Errors stemming from human operation in real experiments could be effectively avoided; (iii) Some expensive experimental raw materials and instruments might fail to meet the research requirements; (iv) Potential pollution associated with some toxic reagents and high-risk instruments to human health and the environment could be avoided; (v) Certain essential thermodynamic and atomic-level structural mechanisms remained elusive through traditional macroscale experimental tests.

Within last ten years, MD has been widely employed in asphalt binder and asphalt mixture systems, including characterization of the molecular properties of the components of asphalt and evaluation of their impact on the overall performance of

asphalt[20-22]; performance investigation or prediction of modified asphalt binder mixed with various modifier (nano metallic oxides, organic polymers, fibers, and organoclay)[23]; evaluation of asphalt self-healing performance and optimization of self-healing schemes[24-26]; analysis of multiple influencing factors in the production, service, maintenance, and regeneration process of asphalt mixtures[27]. By calculating the energy and force interactions between individual components and observing the motions of atoms, molecules, and functional groups in various simulated environments, the performance of asphalt binder and mixture at the micro level could be explored and related to the results obtained from actual experiments. Overall, the application of MD simulation in asphalt binder and mixture could be broadly categorized into the following areas: (i) thermodynamic properties of asphalt molecules; (ii) modification mechanism of modified asphalt binder; (iii) intermolecular interactions between different molecules in asphalt binder; (iv) oxidative reaction of aged asphalt molecules; (v) interfacial interactions between asphalt and aggregate; (vi) self-healing mechanism of asphalt binder or mixture; (vii) impact of asphalt molecular behavior on environment; (viii) rejuvenation effect of aged asphalt. The research hotspots in this field in recent years are shown in Fig. 1.

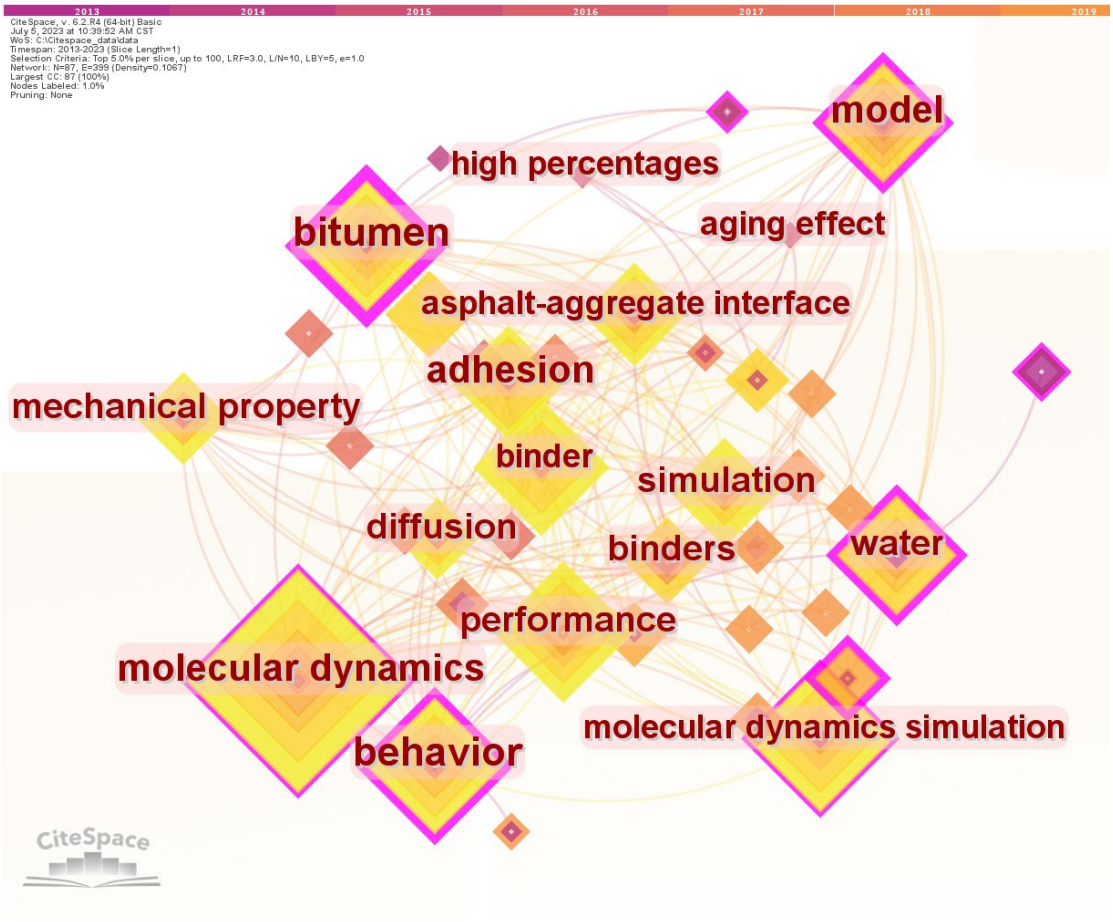

Fig. 1 Research hotspots in asphalt materials by MD simulation.

Several review articles have been published to enhance understanding of the application of MD in realm of asphalt materials. For example, Ren et al., discussed the microscale properties and methodologies of bulk bitumen system form MD comprehensively considering modifying and aging to reveal the potential relationships between nanoscale parameters predicted through MD and macroscale properties measured in experimental tests[28, 29]. Besides, various application cases of MD on asphalt behavior, including diffusion behaviors of oxygen or moisture in asphalt, mobility and distribution of asphalt molecules on aggregate surfaces which notably impacted interfacial bonding levels and moisture sensitivity, micro mechanism and evaluation indices for assessing asphalt self-healing processes, and representative

112 factors influencing the adhesive bonding strength of interfacial models[30]. Yao et al.
113 provided a multi-scale perspective on current studies involving MD of asphalt
114 containing modeling and properties and discussed differences between computational
115 simulation and real samples[31]. Furthermore, Xu et al. reviewed the research
116 progresses in MD of asphalt-aggregate interfaces, including models, estimation factors,
117 affecting status, and interfacial improvements and summarized different models with
118 different compositions, advantages or disadvantages of MD method, feasibility based
119 on quality of MD[32].

120 To our knowledge, no comprehensive review paper has focused specifically on
121 interfacial adhesion of asphalt-aggregate interfaces, delving into the interaction and
122 adsorption mechanisms between them. On the one hand, asphalt-aggregate interface
123 systems are inherently more complex and intricate than individual modified asphalt
124 binder systems. A fundamental interface model comprises at least two components,
125 namely asphalt and aggregate, while some more elaborate models may even include a
126 water layer. The calculation processes and parameters for analyzing interface models
127 differ from those of bulk asphalt models. On the other hand, the number of research
128 articles exploring this aspect has witnessed an exponential growth in the past two years.
129 Therefore, it seems timely to compile recent articles relevant to this field, extracting
130 easily comprehensible information that could guide future researchers investigating the
131 adhesion of asphalt-aggregate interfaces. Such a compilation aims to facilitate access
132 to pertinent content and assist researchers in gaining a deeper understanding of this

topic.

This review delves into the insights gained from MD and discusses the areas where further research is needed to fully understand the complexities of asphalt-aggregate interfaces. It provides a comprehensive overview of the pros and cons of different treatments and evaluations of interfacial properties, ranging from the construction of interface models to the calculation and analysis methods used in MD of asphalt-aggregate interface. It is structured in two parts. The first part describes methods employed for building models of asphalt, aggregates, and interfaces. It also elucidates the process of MD and highlights the calculation parameters used to analyze the simulation results. The second part describes both achievements and open questions concerning the molecular details of different interfacial systems. The main research topics of MD simulation in asphalt-aggregate interfaces and the main content of this review is shown in Fig. 2.

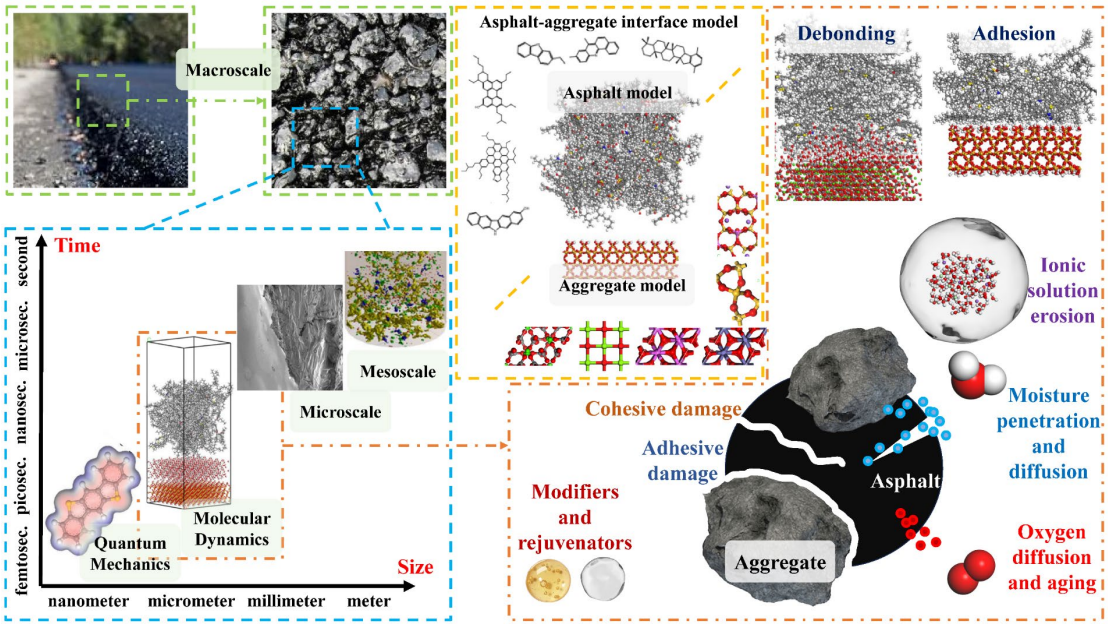

Fig. 2 The research topics and content of this review.

2. Methods of building models

2.1 Asphalt model

Prior to conducting MD simulations, it is essential to establish molecular models for asphalt. Asphalt is an intricate organic mixture, whose specific components are still not fully understood. It comprises a diverse array of organic molecules with varying masses, structures, lengths, polarities, charges, and functional groups, all coalescing to form a viscoelastic material. The chemical composition of asphalt is highly complex, potentially encompassing up to one million different types of molecules. These exhibit a range of functional groups, incorporating heteroatoms such as N/ O /S and cyclic/ aromatic/ saturated hydrocarbons, all combine with large and intricate molecular structures. To simulate asphalt, representative molecules must be carefully selected for system construction. Among the most representative components in asphalt are saturates, aromatics, resins, and asphaltenes[33, 34].

Although there are many chemical representative molecules of asphalt, there is no doubt that twelve component molecules model proposed by Li and Greenfield, as shown in Fig. 3, is the most widely used in MD nowadays[35, 36]. The asphalt molecules are divided into four groups: asphaltenes, polar aromatics (or resins), naphthene aromatics (or aromatics), and saturates. In detail, asphaltenes are composed of three molecules: pyrrole (a1), phenol (a2), and thiophene (a3). Similarly, resin fractions include five molecules: pyridinohopane (pa1), quinolinohopane (pa2), benzobisbenzothiophene (pa3), trimethylbenzene-oxane (pa4), and thio-isorenieratane

(pa5). The aromatics are perhydrophenanthrene-naphthalene (PHPN, na1) and dioctyl-cyclohexane-naphthalene (DOCHN, na2), while saturates are squalane (s1) and hopane (s2). These 12 types of molecules are selected to represent SARA (saturates, aromatics, resins, and asphaltenes) fractions. The number of each type of molecules determine and adjust by experimental data for asphalt speciation and atomic composition in SHRP asphalts. Li and Greenfield also suggested quantities of molecules in three asphalt systems (AAA-1, AAK-1, and AAM-1). Compared to AAA-1, the content of aromatics and resins in AAM-1 is very high but content of saturates and asphaltene is very low. In AAK-1, the largest difference of molecular ratio is the dosage of saturates reduced by 50%. Unfortunately, the simulation results of AAM-1 and AAK-1 are not so close to the experimental values as those of AAA-1.

Apart from the AAA-1 asphalt models, several other researchers have utilized twelve asphalt models to construct different virgin asphalt systems, such as QL-90#[37] and PG 64-16[38], as well as AAK-1 and AAM-1[39]. In addition, representative molecules based on twelve molecules of SARA components can also be more specifically subdivided. Different asphalt derived from various oil sources can be subdivided into distinct representative molecules, although these representative molecules might not differ significantly from the 12 molecules of AAA-1. For instance, all asphaltene models exhibit continuous islands aromatic ring structures[40, 41]. By using similar molecules to represent the SARA components and fine-tuning some representative molecules, researchers have created more representative molecular

structures. This has led to an increase in the number of representative molecules to 16, 19, or even more[22]. The establishment of these models is based on the following fundamental logic: combining the results of four-component tests conducted on different types of asphalt with data obtained from techniques such as FTIR, GPC, GC-MS results, and the number of asphalt molecular models is adjusted so that four component results of the model align with the test results.

The oxidative aging process of AAA-1 asphalt molecules was investigated by ReaxFF in LAMMPS to predict the locations and formation rules of oxygen-containing functional groups after aging[42]. Quantitative analysis of oxidation products like ketones and sulfoxides are used to confirm the feasibility of coordination between asphalt molecules and atomic oxygen to represent the oxidation process. It is observed that generation of S=O is earlier than generation of C=O. In addition, C=O are more readily generated on cyclic benzyl carbons compared to branched benzyl carbons. Sulfur atoms in asphaltenes and resins are found to predominantly form S=O, while carbon atoms separated from the benzene rings in asphaltenes, resins, and aromatics are more susceptible to attack by oxygen molecules, resulting in formation of C=O[43]. Different aging durations lead to the formation of distinct polar oxygen-contained functional groups. In brief, the variation in aged asphalt molecule structures, representing different aging durations, primarily reside in the presence of S=O and C=O. A short-term aged asphalt model, focusing solely on the formation of S=O, is constructed to represent the initial aging process[25, 44]. Ren et al. divided aged asphalt

molecules into two to four different groups based on aging times and degrees, which correlated with varying amounts of oxygen-containing functional groups[45]. Qu et al. also proposed the short-term and long-term aged asphalt models, considering different positions and amounts of C=O and S=O, fully accounting for the chemical properties of asphalt binder at different aging stages[46]. Xu and Wang introduced full-oxidative aged asphalt molecular models and discovered that oxidative aging increased density, viscosity, and CED, but reduced SFE as well as weakened the aggregation behavior and translational mobility of asphalt molecules[47]. Consequently, the composition and quantity of aged asphalt molecules were ultimately determined, as listed in Table 1[48].

Table 1 Molecules of virgin and aged asphalt of AAA-1.

Molecular	Virgin asphalt		Aged asphalt	
	Formula	Number	Formula	Number
Squalane (s1)	$C_{30}H_{62}$	4	$C_{30}H_{62}$	5
Hopane (s2)	$C_{35}H_{62}$	4	$C_{35}H_{62}$	6
PHPN (na1)	$C_{35}H_{44}$	11	$C_{35}H_{36}O_4$	9
DOCHN (na2)	$C_{30}H_{46}$	13	$C_{30}H_{42}O_2$	10
Quinolinohopane (pa1)	$C_{40}H_{59}N$	4	$C_{40}H_{55}NO_2$	6
Thioisorenieratane (pa2)	$C_{40}H_{60}S$	4	$C_{40}H_{56}O_3S$	6
Benzobisbenzothiophene (pa3)	$C_{18}H_{10}S_2$	15	$C_{18}H_{10}O_2S_2$	18
Pyridinohopane (pa4)	$C_{36}H_{57}N$	4	$C_{36}H_{53}NO_2$	6

Trimethylbenzeneoxane (pa5)	$C_{29}H_{50}O$	5	$C_{29}H_{48}O_2$	7
Asphaltene-phenol (a1)	$C_{42}H_{54}O$	3	$C_{42}H_{46}O_5$	5
Asphaltene-pyrrole (a2)	$C_{66}H_{81}N$	2	$C_{66}H_{67}NO_7$	4
Asphaltene-thiophene (a3)	$C_{51}H_{62}S$	3	$C_{51}H_{54}O_5S$	5

221

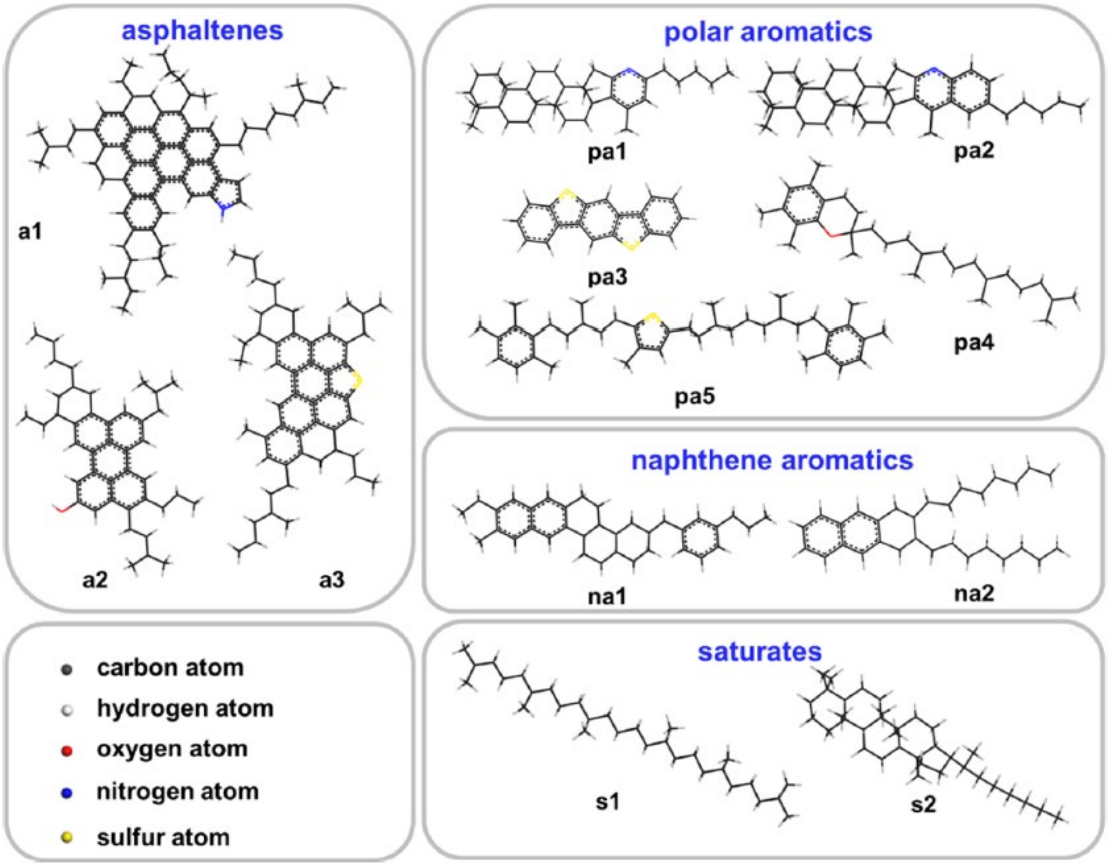

222

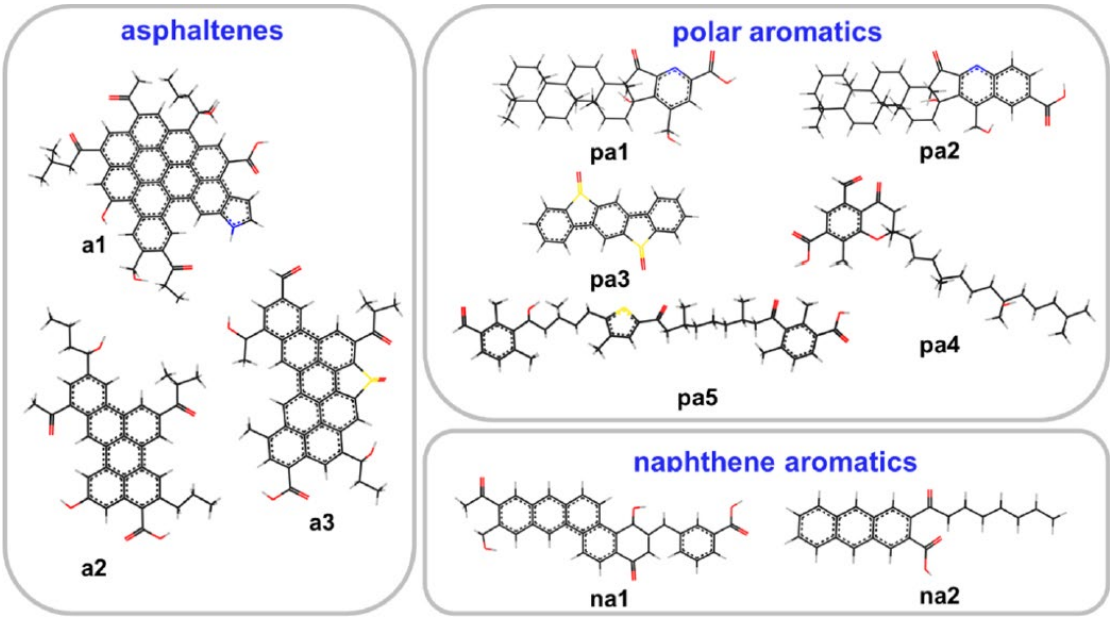

Fig. 3 Twelve-components molecular models of unaged and aged base asphalt[49].

In addition to the most widely employed twelve molecule model, three component and four component models were also utilized in the early stages of asphalt MD simulation. However, with a reduced number of components, the complexity of the asphalt system decreases, leading to diminished representativeness of each component. However, it is generally no longer recommended to use simplistic models when more realistic molecular component models are available. Examples of several three component and four component molecular models are as follows in Fig. 4.

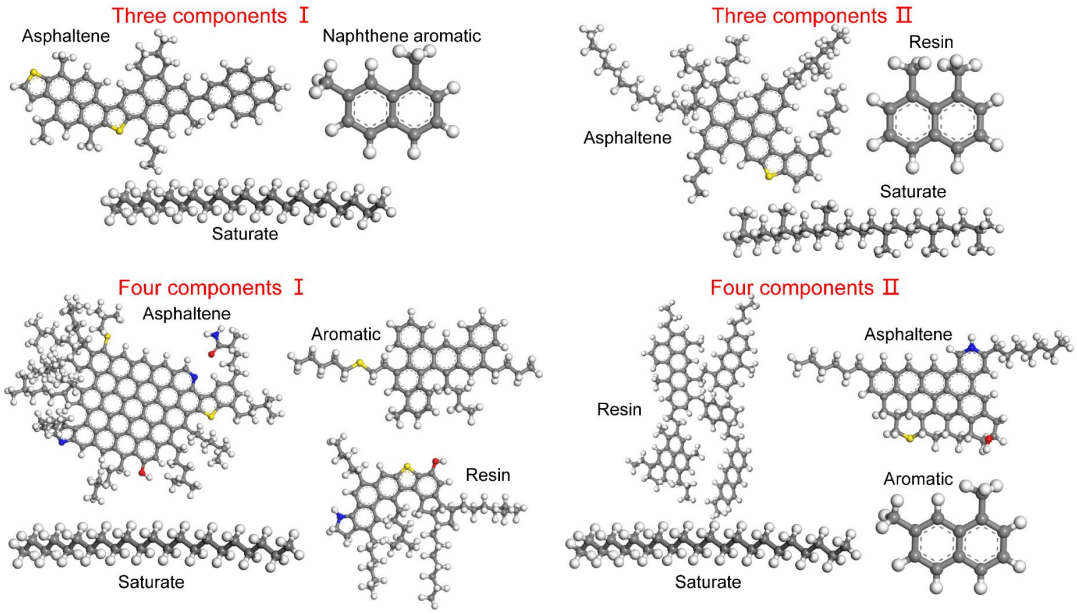

Fig. 4 Three component molecules model I: saturate ($C_{22}H_{46}$), naphthene aromatic ($C_{12}H_{12}$), asphaltene ($C_{64}H_{52}S_2$)[50-52]; Three component molecules model II: Saturate ($C_{30}H_{62}$), resin ($C_{12}H_{12}$), asphaltene ($C_{72}H_{98}S$)[53, 54]; Four component molecules model I: saturate ($C_{22}H_{46}$), aromatic ($C_{46}H_{50}S$), resin ($C_{59}H_{85}NOS$), asphaltene ($C_{149}H_{177}N_3O_2S_2$); Four component molecules model II: saturate ($C_{22}H_{46}$), aromatic ($C_{12}H_{12}$), resin ($C_{100}H_{106}$), asphaltene ($C_{53}H_{57}NOS$)[55].

2.2 Aggregate model

In practical asphalt road engineering, granite, basalt, sandstone, diabase, and limestone are commonly used. The main chemical composition of granite and basalt is silica (SiO_2) which are weakly acidic. Meanwhile, limestone is mainly composed of calcite ($CaCO_3$). Additionally, some other types of aggregates could be applied in pavement for meeting special requirements, including metal oxides and steel slag. Limestone, for example, is a sedimentary rock primarily composed of $CaCO_3$, which forms from the accumulation of marine organisms such as shells and coral. Basalt, on

247 the other hand, is an igneous rock formed from the solidification of molten lava. It is
248 typically rich in minerals such as pyroxene, plagioclase, and olivine, which give it its
249 characteristic dark color and fine-grained texture. Sandstones, like limestone, are
250 sedimentary rocks that are primarily composed of sand-sized grains of mineral, rock,
251 or organic material. Diabase is a type of intrusive igneous rock that forms from the slow
252 crystallization of magma deep beneath the Earth's surface. It is typically composed of
253 plagioclase feldspar, pyroxene, and sometimes olivine, and is known for its dark, fine-
254 grained texture. Granite is perhaps the most well-known of these formations, and for
255 good reason. This coarse-grained igneous rock is typically composed of quartz (SiO_2),
256 feldspar, and mica.

257 As we known, the rock or stone is a complex mixture contained a lot of different
258 components, including a large amount of crystals and amorphous or non-crystals. To
259 simulate the completely real model of aggregate is an impossible goal because the micro
260 contact areas at angstrom scale would restrict the presentation of overall morphology
261 of stone. The models of aggregates used in simulation process must be ideal and
262 representative samples. For example, the oxides of basalt are ranked as: $SiO_2 > Al_2O_3 >$
263 $Fe_2O_3 \approx CaO \approx MgO$[56, 57], while of limestone are $CaCO_3$, SiO_2, Al_2O_3, Fe_2O_3, CaO,
264 and MgO[58]. The common aggregate models are listed in Table 2, including their
265 chemical formula and lattice parameters.

266 Table 2 The chemical formulas and crystal structure of the representative minerals[59-
267 61].

Mineral	Chemical formula	Space group	Lattice length/ Å	Lattice angle/ °
Quartz	SiO_2	$P3_221$	a=b=4.90, c=5.40	α=β=90, γ=120
Calcite	$CaCO_3$	$R\bar{3}C$	a=b=4.98, c=16.99	α=β=90, γ=120
Chlorite	$Mg_3Al_2Si_4O_{18}$	C2/c	a=5.22, b=9.06, c=28.38	α=γ=90, β=93.7
Mica/Muscovite	$NaAl_2Si_4O_{12}$	C2/c	a=5.19, b=9.00, c=20.10	α=β=γ=90
Pyroxene/Augite	$FeMgSi_2O_6$	C2/c	a=9.73, b=8.91, c=5.27	α=γ=90, β=106.82
Montmorillonite	$CaAl_2Si_4O_{12}$	C2/m	a=5.18, b=8.98, c=15.00	α=β=γ=90
Alkalifeldspar/Albite	$NaAlSi_3O_8$	$P\bar{1}$	a=8.12, b=12.76, c=7.16	α=94.21, β=116.8, γ=87.71

Microcline	$KAlSi_3O_8$	$P\bar{1}$	a=8.57, b=12.96, c=7.22	α=90.57, β=115.92, γ=87.75
Plagioclase/Anorthite	$CaAl_2Si_2O_8$	$P\bar{1}$	a=8.19, b=12.88, c=14.18	α=93.3, β=115.79, γ=91.12
Nepheline	$(Na,K)AlSiO_4$	$P6_3$	a=b=10.00, c=8.38	α=β=γ=90
Calcium oxide	CaO	$Fm\bar{3}m$	a=b=c=4.81	α=β=γ=90
Magnesium oxide	MgO	$Fm\bar{3}m$	a=b=c=4.21	α=β=γ=90
alumina	Al_2O_3	$R\bar{3}C$	a=b=4.76, c=12.99	α=β=90, γ=120
Ferric oxide	Fe_2O_3	$R\bar{3}C$	a=b=5.04, c=13.72	α=β=90, γ=120
Diopside	$CaMgSi_2O_6$	C2/c	a=9.79, b=8.96, c=5.25	α=γ=90, β=105.37
Forsterite	Mg_2SiO_4	Pnma	a=4.67, b=10.20, c=5.98	α=β=γ=90
Steel slag (C2S,	$Ca_2Si_2O_6$	P21/n	a=9.88,	α=γ=90,

dicalcium silicate)		b=8.91, c=5.22	β=103.7
Steel slag (C3S, tricalcium silicate)	Ca_3SiO_5	$P6_3/mmc$	a=b=5.15, c=10.17	α=β=90, γ=120

The aggregate model construction method can be divided into three steps: (i) selecting the suitable crystal unit cell and cleaving it in an appropriate direction. For instance, the SiO_2 and $CaCO_3$ are usually cleaved in (0,0,1) and (1,0,4) directions respectively. The thickness of cleaved crystal is determined by certain research requirements; (ii) Establishing the supercell surface in x- and y- directions by adapting the size of asphalt model to obtained aggregate layer. If necessary, the terminating hydroxyl (-OH) group can be added to contact surface; (iii) Constructing a vacuum layer with a thickness of 1 or 0 Å to ensure the aggregate structure in periodic boundary conditions. This step is to make sure that aggregate layer can form in interfaces as an independent entity. After these construction steps, a geometry optimization process should be run in aggregate model.

2.3 Asphalt-aggregate interfacial model

The asphalt-aggregate interfacial model is constructed by piling asphalt layer model above aggregate layer. To satisfy the periodic boundary condition, a vacuum layer is incorporated upon asphalt layer model. A geometry optimization step is usually conducted before running dynamics process. Generally, the mineral models are introduced by complete cases, so it is not necessary to optimize structures of aggregates

individually but optimize interfaces models integrally. Then, forcefield, time step, ensemble, temperature, and total number of steps are selected for performing dynamics procedure. In general, the energy summation of Van der Waals and electrostatic energies are recommended to use Atom-based and Ewald methods, respectively. Some chemical bonds such as bonds that represented connection between anions and cations should be deleted after construction of interfaces.

When determining the size of the interface model, computational resources need to be taken into account. The larger the size of the model, the higher the accuracy of the final calculation results, and the longer the dynamic calculation process. A model with a plane size of 100 Å * 100 Å in the x- and y- direction should have a much smaller error in multiple calculations compared to a model with a size of 40 Å * 40 Å interface model. Choosing a time step that is too small would consume excessive computer resources and limit the duration of the MD, while a time step that is too large could lead to rapid energy increase over time and render the MD unstable. Therefore, the time steps in MD of asphalt materials are commonly set to 1.0 fs. Similarly, the cutoff distance is commonly set to 15.5 Å, taking into consideration the same trade-off between accuracy and computational efficiency.

3. Interfacial properties between asphalt-aggregate

3.1 Binding or adhesion energy of interface

The interfacial adhesion has been investigated through direct simulation methods, focusing on calculating the work or energy of adhesion. Researchers have constructed

306 interface structures between asphalt and different aggregates to explore their adhesion
307 properties. In MD studies, if the aggregate was decomposed into metal oxides, the
308 interfacial adhesion work was ranked as follows: Al_2O_3 >Fe_2O_3 >CaO >MgO >SiO_2,
309 with the influence of mineral types being more significant compared to asphalt types.
310 Van der Waals energies predominantly contributed to adhesion for SiO_2, CaO and MgO,
311 while Coulomb electrostatic energy played a greater role for Al_2O_3 and Fe_2O_3.
312 Moreover, the diffusion of asphalt on alkaline mineral is larger than that of natural and
313 acid mineral, with an stronger alkaline strength leading to increased interfacial
314 adhesion[62].

315 The work of adhesion with asphalt varied among different aggregates, with quartz
316 < anorthite < albite < muscovite < chlorite < augite. These variations in adhesion work
317 likely explain the predominant influence of aggregate properties on asphalt-aggregate
318 interactions. In asphalt colloid, the concept of selective adsorption suggests that exhibit
319 a preference for adsorption onto aggregate surfaces owing to their high polarity, while
320 aromatics and saturates display a contrary trend. This selective adsorption leads to
321 direct contact between asphaltene molecules and aggregate surfaces, while aromatic
322 and saturate molecules primarily distributed in the outermost layer. The resins act as
323 structural skeleton, along with stabilizers to improve compatibility between asphaltenes
324 and nonpolar molecules. Besides, the aromatics fill intermolecular gaps, while saturates
325 lubricated molecular micelles. The AFM results showed that polar components
326 agglomerate into boundaries and avoid the center of lower adhesion force regions at

interfaces. The dissolution of polar molecules into water resulted in collapse of nanostructure, followed by subsequent debonding at asphalt-aggregate interfaces[63].

3.2 Failure of interface

An alternative approach to investigate the intermolecular effect between asphalt and aggregates involves conducting compression or shear simulations under varying pressures, temperatures, and shear velocities[50, 64]. The resistance of asphalt molecules to stress-strain failure determines the cohesion of asphalt under compressive and shear stresses. Likewise, stronger adhesion abilities at asphalt-aggregate interfaces result in reduced molecular displacement or separation under stress. Applying pressure to asphalt near the interface leads to noticeable stratification along interface direction, with greater pressure causing faster variation between asphalt and aggregate. Some oxide mineral aggregates containing multiple metal elements, such as anorthite ($CaAl_2Si_2O_8$), augite ($FeMgSi_2O_6$), and albite ($NaAlSi_3O_8$), form a lubrication layer with diffused metal ions, causing asphaltene disaggregation, instability of asphalt colloidal structure, and reduced resistance under substrate shearing[64]. Contact opportunities between free metal ions and asphalt molecules increase under compressive or shear stress, penetrating deeper into asphalt and damaging its colloidal structure. Modeling the aggregate-asphalt-aggregate system allows exploring contribution of relative molecular mass and component content to performances of asphalt mixtures, where higher relative molecular mass and resin content result in a larger shear modulus and higher shear strength. The adhesion of interfaces during

348 confined shear is significantly influenced by asphaltene[65].

349 Furthermore, a simulated pull-off test can be employed to analyze interfacial
350 failure patterns and mechanisms. A typical process of pull-off test at asphalt-aggregate
351 interface in MD is shown in Fig. 5 (a) while the typical failure types of interfaces are
352 presented in Fig. 5 (b). The tensile simulations of a well equilibrated system were
353 conducted using the fix velocity method within NVE ensemble. This approach
354 facilitated the evaluation of the system's response to tensile forces and provided insights
355 into the stress distribution along the z-axis. Factors such as aggregate types, aging state
356 of asphalt, loading rate, and temperature influence adhesion properties at asphalt-
357 aggregate interfaces, as presented in Fig. 5 (c) and (d). Under specified conditions,
358 separation at asphalt-aggregate interfaces primarily occurred within asphalt regions,
359 suggesting a stronger adhesive strength than cohesive strength in asphalt. In severely
360 aged asphalt, the cohesive strength surpassed interfacial adhesion, resulting in
361 debonding on aggregate surfaces. Aging of asphalt leads to stronger tensile strength so
362 that resist to fracture, while molecular agglomeration of asphalt reduces the flowability,
363 causing suffering fatigue failure more easily. The adhesive failure predominated at
364 interfaces, although bulk asphalt may contain air voids at lower loading rates[66, 67].
365 The extension rate of pull-off test played a crucial role in determining failure
366 mechanism of asphalt-aggregate interfaces, with adhesive failure at a small extension
367 rate and cohesive failure at a larger extension rate in asphalt-SiO_2 system[68]. The
368 percentage of cohesive debonding at asphalt-calcite interfaces increased with thicker

asphalt films, lower loading velocities, and higher temperatures[69]. Except for external factors, the failure mode depended on asphalt internal interaction and asphalt-aggregate interfacial interaction, where cohesive failure occurred when binding energy between asphalt and aggregate molecules exceeded cohesive energy of asphalt. Stronger adhesion between asphalt and aggregates reduced likelihood of interfacial separation in pull-off test.

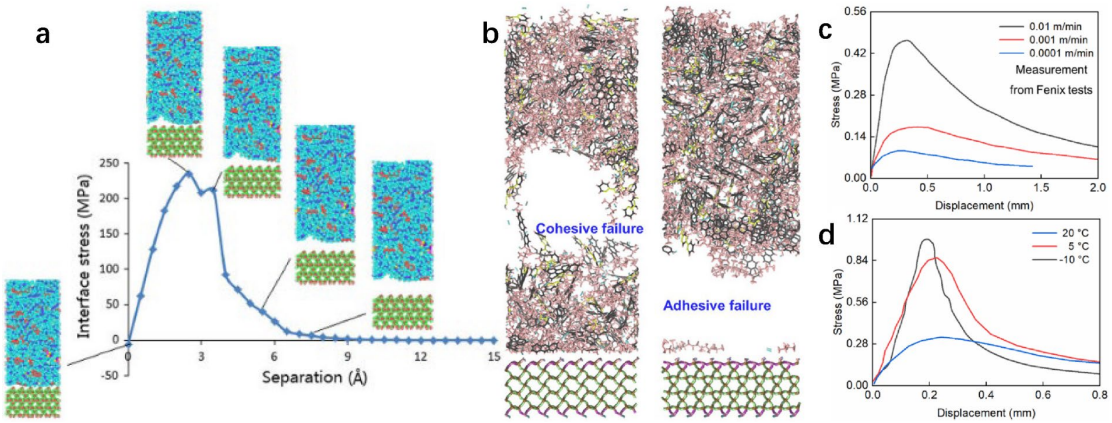

Fig. 5 Pull-off test in MD simulation: (a) typical prediction of tensile stress at interface[70]; (b) cohesive and adhesive failure of asphalt-SiO_2; (c) and (d) stress–displacement relationship at different loading rates and temperatures[49].

3.3 Contact between asphalt and aggregate

The evaluation of wettability at asphalt-aggregate interfaces through contact angle measurements provides insight into molecular strength between asphalt and aggregate upon contact. As demonstrated in Fig. 6 (a) and (b), smaller contact angle indicates higher potential for asphalt droplet wetting on aggregate surfaces, reflecting stronger molecular affinity. The contact angle serves as a means to compare adhesion across various interfaces. A smaller contact angle signifies that aggregate surface has an

affinity for asphalt droplet. Conversely, a greater contact angle suggests a weaker molecular attraction at asphalt-aggregate interfaces. In addition to interactions between asphalt and aggregates, the contact angle largely depends on status of asphalt droplets. As shown in figures, as temperature increases, asphalt exhibits a softening characteristic at macro level, leading to a larger contact area and enhances contact between asphalt and aggregate surface. At the same time, the increase in temperature makes movement of asphalt molecules more active, resulting in closer contact between asphalt and aggregate surface. Furthermore, the contact angle is influenced by properties of asphalt and aggregates. The experimental results of various asphalt and aggregates obtained through contact angle test are shown in the Fig. 6 (c). The variations in contact angle were observed between different aggregates on same surface or with same asphalt on different surfaces[71, 72]. Furthermore, the contact angles for asphalt with limestone, diorite, diabase, and steel slag surfaces obtained by experimental test are shown in Fig. 6 (e)-(h), respectively.

However, the significant scale difference between actual contact angle tests (centimeter level) and simulation (nanometer level) may result in discrepancies between experimental and simulated values. Excessive scale differences may lead to significant differences between experimental and simulated values. On the other hand, contact angle values obtained from simulations by measuring asphalt molecular droplets primarily represent angle between plane where outermost molecules within asphalt droplet are located and plane where molecules reside on aggregate surface. This

largely depends on the composition and structure of molecules around asphalt droplets and on aggregate surfaces. Considering the intricate nature of asphalt and aggregate, researchers are constrained to select representative molecular structures that closely resemble real-world scenarios when conducting simulations. However, this approach does not guarantee perfect alignment between simulated contact angles and numerical values obtained from experiments. The challenge arises from the difficulty in precisely determining the specific composition and structure of the aggregate surface at point of contact with edge of asphalt droplet during actual contact angle measurements. Fortunately, this discrepancy offers an avenue for future investigations. By continuously adjusting the composition and structure of asphalt droplet and aggregate surface molecules, researchers can strive to attain contact angle values in simulations that closely align with and match values obtained in experimental settings. This iterative process aims to enhance the accuracy of asphalt-aggregate interface models.

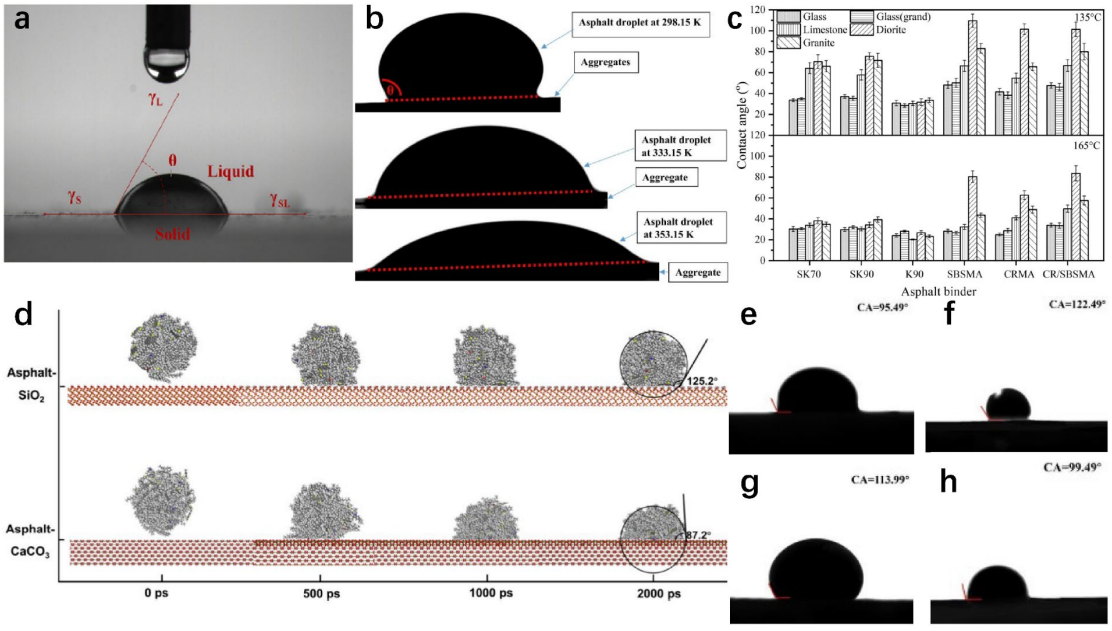

Fig. 6 Water contact angle measurement: (a) schematic diagram of contact angle

method; (b) asphalt droplet on aggregates at different temperatures[73]; (c) contact angle of asphalt binders on different surfaces[74]; (d) wetting process of asphalt on SiO_2 and $CaCO_3$[71]; (e)-(h) contact angle of bitumen with limestone, diorite, diabase, and steel slag[75].

The role of surface roughness in aggregate is crucial for interfacial adhesion, with various surface nanostructure patterns such as grooves, grids, and pillars being generated to achieve predefined roughness ratios in aggregate models. The surface nanostructure plays an important role in interaction energy, tensile bond strength, and interlocking. The surface roughness promotes adsorption of asphalt chains, reinforcing interlocking and reducing adhesive failure[76]. The work of adhesion experiences a significant increase as surface irregularity radius expands, indicating a strengthened adhesion strength with heightened aggregate surface roughness. This can be attributed to the creation of more potential interacting sites on aggregate surfaces, leading to a notable enhancement in bonding strength at asphalt-aggregate interfaces. Notably, the rise in adhesive work with surface irregularity radius primarily arises from escalation of van der Waals, while electrostatic remains relatively unaffected[77].

3.4 Characteristics of asphalt molecules

The interfacial adhesion in asphalt-aggregate systems is influenced by the nature of four-component molecules in asphalt, including their weight, volume, polarity, and aromaticity. Moreover, the compositions and spatial-temporal distributions of these molecules within interfacial zone also play a crucial role in interfacial adhesion[78].

Specifically, polarity of asphalt components is the most important in influencing interfacial adhesion. The polarity of asphalt components in followed an order of asphaltenes > resins > aromatics > saturates. Asphaltenes and resins exhibit higher polarity due to the presence of heteroatoms (N, O, S) and continuous benzene rings, resulting in uneven charge distributions within these polar asphalt molecules. The interaction composition between polar and non-polar components primarily influences interface adhesion. Saturates and aromatics, as non-polar components, primarily rely on van der Waals forces for adsorption onto aggregate surfaces due to their smaller molecular weights. Meanwhile, resins and asphaltenes, as polar components with larger molecular weights, contain a significant amount of polar groups. These polar groups exhibit chemical reactivity and contribute to adhesion through not only van der Waals but also electrostatic forces in interaction between these components and interfaces. Asphaltic acids and anhydrides allow for chemisorption, which forms strong bonds with active centers on aggregate surfaces and is challenging to desorb. Consequently, the adhesion between asphalt components and mineral aggregates is favorable. The adhesion at interfaces between non-polar saturates/ aromatics and polar mineral molecules is less effective due to the strong polarity of mineral surface, reducing surface tension and causing poor adhesion. Thus, the interfacial adhesion to aggregate of saturates/ aromatics and is lower than that of asphaltene/ resin[79]. Overall, van der Waals forces predominantly govern the interactions between asphalt and aggregates. Benzene rings and heteroatoms in polar components facilitate van der Waals

464 interactions, while additional electrostatic interactions and hydrogen bonds between H
465 and O/ N contained functional groups contribute to increased free energies and forces
466 at asphalt-aggregate interfaces. The van der Waals, electrostatic, and hydrogen bonds
467 exist during interactions between polar asphalt molecules and aggregates.
468 Simultaneously, the binding energies between asphalt and aggregates also increase with
469 higher polarity, demonstrating the significance of polarity in asphalt-aggregate
470 interactions[80].

471 In the context of different mineral compositions, the adhesion behavior is
472 primarily governed by Van der Waals interactions. This result is related to asphalt
473 compositions from different sources. While the sequence of adhesion work showed
474 variations in certain cases, suggesting that adhesion is not solely determined by Van der
475 Waals. Therefore, the electrostatic interaction were identified as a significant factor
476 influencing adhesion work between different types of asphalt and same aggregate[81].
477 The adhesion was strongly influenced by proportion of asphaltenes/ polar components
478 in asphalt, wherein higher asphaltene content and density resulted in improved cohesion
479 and greater crack resistance. Variations in content of SARA components affected
480 colloidal structure and internal morphology of asphalt, ultimately impacting initiation
481 location of nanovoids. Further examining of distribution of asphalt components
482 indicated that local nanostructure played a role in molecular mechanical behavior.
483 Regions with lower concentrations of polar molecules and heteroatoms were found to
484 be more prone to nanovoid initiation. Furthermore, during tensile deformation,

asphaltene atoms experienced greater atomic forces compared to maltene atoms[82]. The interfacial adhesion work increased as fractions of asphaltene and resin in asphalt increased[83, 84].

Asphaltenes play an important role in asphalt-aggregate interface interaction[85]. As the average structure $C_{65}H_{74}N_2S_2$ as representative molecular of asphaltenes, the interfacial energy between asphaltenes and MgO is the greatest, followed by CaO, Al_2O_3, and SiO_2, revealing that interaction with alkaline aggregates is superior to acidic aggregates[86]. Both electrostatic and van der Waals energies contribute to binding energy of asphaltene-aggregate interfaces, surpassing other three asphalt components. This is primarily due to higher polarity and average molecular weight of asphaltene, along with a greater number of atoms compared to other components. The presence of heteroatoms and polar functional groups in asphaltenes, as well as π-π stacking between benzene rings in asphaltenes, significantly influence adhesion of asphalt-aggregate interfaces[87]. The Fig. 7 (a)-(e) showed the positive and negative electron density of asphalt molecules. Electron density analyses demonstrated that larger differences in charge density result in stronger attractions. The continuous island aromatic ring structure in asphaltene facilitates parallel arrangements between asphaltene molecules and promotes alignment parallel to aggregate surfaces due to mutual attraction between positive and negative electrons, as shown in Fig. 7 (f). Furthermore, the adhesion properties of asphaltene are enhanced by hydrogen bonding and covalent bond breaking. Despite relatively low proportion of asphaltene in asphalt binder (10%), it substantially

contributes to adhesion properties between binder and aggregates[88].

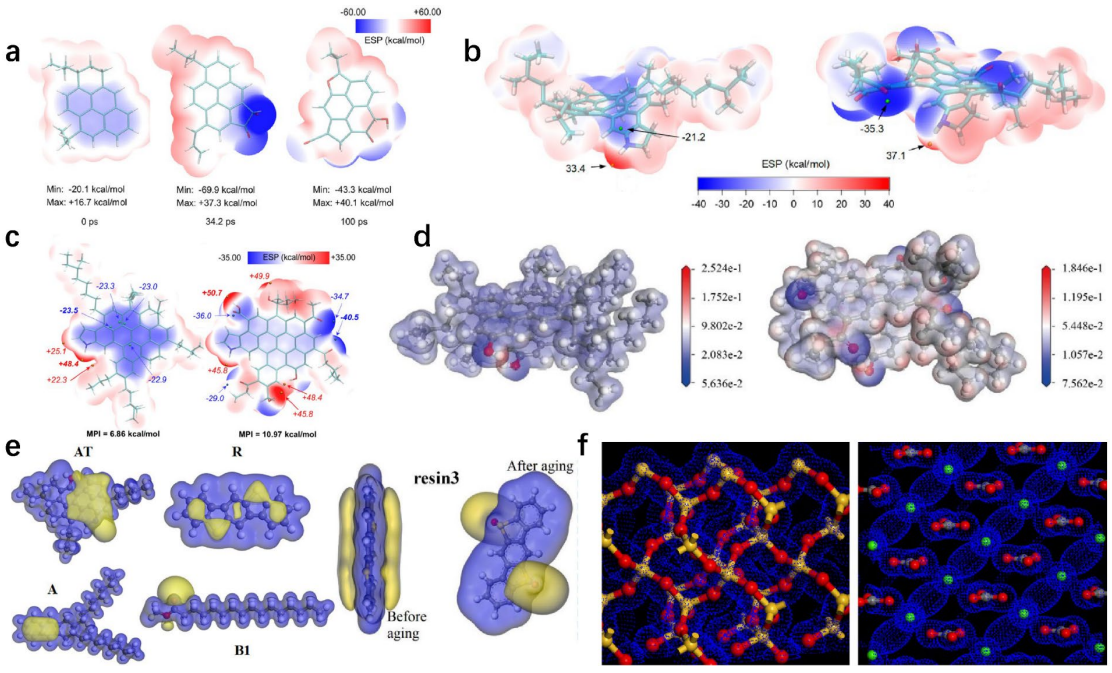

Fig. 7 Electrostatic potential isosurface maps: (a) asphaltene molecules with different aging degrees[89]; (b) and (c) virgin and aged asphaltene molecules[49, 90]; (d) virgin and aged asphaltene dimer[91]; (e) electronic charge of asphalt molecules[92, 93]; (f) electron densities of α-quartz and calcite crystals[94].

3.5 Influence of different aggregates

3.5.1 Different minerals

The types and characteristics of aggregates have a significant impact on adhesion at asphalt-aggregate interfaces. Aggregates are commonly categorized as acidic (e.g., silica) or alkaline (e.g., calcite), while neutral aggregates like alumina have also been studied. In the early days of using MD to study adhesion, researchers mostly only constructed simple asphalt-SiO_2 and asphalt-$CaCO_3$ interfaces. The chemical compositions of aggregates play crucial roles in interface adhesion, as different

chemical structures yield distinct computational values during simulation. This is the basis for exploring interfacial adhesion differences through simulation.

Van der Waals and electrostatic forces are key contributors to interface adhesion, with compositions of aggregates influencing their relative importance. Van der Waals forces primarily contribute to cohesion of asphalt, while adhesion between asphalt and aggregates is significantly influenced by mineral types both under dry and wet conditions. For compounds mainly composed of covalent bond, van der Waals force is the most important combination of asphalt and aggregate. Ionic compounds or ionic crystals like CaO and MgO exhibit the highest electrostatic energy due to formation of ionic bonds between metal cations and oxygen anions through electrostatic interaction[95]. In the case of α-quartz, the electron density uniformly distributes along Si-O bonds, implying relatively stable covalent bonds between silicon and oxygen. Conversely, calcite exhibited a localized reduction in electron density between Ca^{2+} and CO_3^{2-} ions, indicating weaker ion bonds between Ca^{2+} and CO_3^{2-} compared to electron-sharing covalent bonds within CO_3^{2-} ions. Consequently, cleaving the surface of calcite would result in the rupture of ion bonds between Ca^{2+} and CO_3^{2-} ions while preserving the covalent bonds within CO_3^{2-} ions. Under dry conditions, asphaltenes/ resins tended to accumulate nearer surface of calcite aggregate than aromatics/ saturates due to potential charge interactions[96]. Furthermore, metallic elements in aggregates were adsorbed by asphalt due to cation–π interaction between electron-rich π aromatic plane of asphalt and metal or due to strong coulomb interactions between metallic ions and

polar functional groups[97, 98].

Aggregate types have a greater impact on adhesion between modified asphalt and aggregates compared to asphalt types. As shown in Fig. 8 (a)-(c), the adhesion of asphalt-aggregate interfaces could be evaluated by concentration distribution, adhesive work, and bonding ratio. From an energy perspective, strong alkali aggregates have large electrostatic interaction with asphalt, while van der Waals energy only contributes a little[99]. Under both dry and wet conditions, adhesion and debonding works to asphalt of alkali mineral are higher than acid mineral. The adhesion of interface is dominated by non-bond interaction energies, with primary component being van der Waals for acid minerals and electrostatic for alkali minerals. The asphalt-aggregate debonding is a thermodynamically favorable process, resulting in a decrease in total potential energy of system[100]. Fig. 8 (d) shows different interfaces of asphalt with different aggregate models[59, 60]. Similarly, limestone, granite, and basalt-asphalt interfaces could be observed by SEM images as shown in Fig. 8 (e). The stronger interaction between asphalt and aggregates leads to molecule aggregation and rotation near surfaces, as well as a gradient distribution of asphalt molecules perpendicular to surface. The observed higher value of total diffusion to diffusion in the z-direction indicates reduced mobility of asphalt molecules perpendicular to surface, which is likely attributed to enhanced adsorption, as presented in Fig. 8 (f).

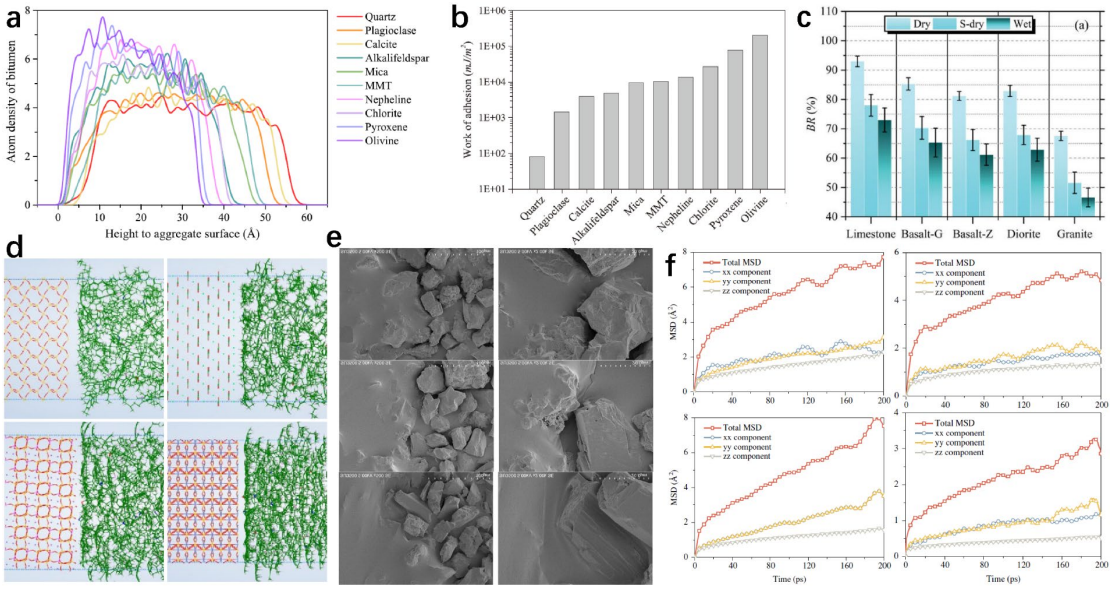

Fig. 8 Adhesion of asphalt-aggregate interfaces: (a) atom density of asphalt on aggregates; (b) work of asphalt-mineral adhesion[60]; (c) bonding ratio between asphalt and aggregates[101]; (d) adsorption of asphalt on quartz, calcite, alkalifeldspar, and pyroxene surface; (e) SEM images for limestone, granite, and basalt-asphalt interface[102]; (f) MSD of the asphalt on anorthite, albite, muscovite, and chlorite surfaces[59].

3.5.2 Different cleave surfaces and hydrogen bonds

The interfacial adhesion is influenced by different cleaving surfaces. The exposed α-quartz and calcite surfaces, including (001), (100), and (101) for α-quartz and (104), (214), and (018) for calcite were investigated. The adhesion energy rankings with asphalt were found to be (101) > (100) > (001) for α-quartz and (018) > (214) > (104) for calcite. The adhesion mechanism is strongly correlated with atomic density of mineral surface and presence of dangling bonds from surface active ions. Calcite exhibit stronger bonding strength with asphalt compared to α-quartz[94]. The adhesion work

575 shows consistent trends in Van der Waals energy, with CaO > Al_2O_3 > SiO_2. In total
576 adhesion work, van der Waals force accounted for over 90% in cases of CaO and SiO_2,
577 while Coulomb force contributed more than 70% in case of Al_2O_3. Moreover, variations
578 in cleaving surface and hydroxylation degree led to different interfacial properties. For
579 SiO_2, the adhesion energy rankings with asphalt were (001) > (100) > (011)[81].
580 Furthermore, in albite aggregate model, the electrostatic adsorption capacity was
581 significantly stronger for (100) surface compared to (001) surface[103].

582 The asphalt-SiO_2 interaction is predominantly attributed to non-bond interactions,
583 indicating absence of significant chemical reactions and covalent bonding. The non-
584 bond interactions are primarily governed by van der Waals, while electrostatic plays a
585 negligible role in asphalt-SiO_2 interactions. This is expected, as it is challenging to form
586 electrostatic interactions between asphalt and electrically neutral mineral[104].
587 However, the introduction of hydroxyl groups on the α-quartz surface led to
588 electrostatic attraction to asphalt binder. Based on results of real pull-off tests, the bond
589 strength at asphalt-aggregate interfaces, considering both aggregate properties and
590 asphalt binder properties, could be summarized as follows: (i) calcite and limestone
591 exhibited superior bonding properties with asphalt binder compared to basalt; (ii)
592 asphalt with more polar components or those subjected to aging demonstrated stronger
593 adhesion to aggregates[105].

594 Besides van der Waals and electrostatic, the interactions involving polar
595 components on aggregate surfaces have been extensively examined. Notably, the

596 presence of hydrogen bonding interactions has been identified as a significant
597 contributor to the overall adhesion energy[106]. Hydrogen bonds are characterized as
598 weak interactions formed between hydrogen and electronegative atoms such as nitrogen,
599 oxygen, and fluorine. Hydrogen bonds schematic diagram can be demonstrated in Fig.
600 9 (a).

601 In asphalt-quartz interfaces, hydrogen bonds are observed between O atoms in
602 SiO_2 and polar asphalt molecules. It is noted that all hydrogen bond lengths exceeded
603 3 Å. On the other hand, as shown in Fig. 9 (b), in asphalt-calcite systems, the hydrogen
604 bonds occurred between CO_3^{2-} and polar asphalt molecules exhibit significantly greater
605 strength compared to the asphalt-α-quartz systems. This is attributed to smaller H bond-
606 lengths and bigger bond-angles observed in asphalt-calcite systems. However, it is
607 found that contribution of hydrogen bond interactions is relatively minor compared to
608 van der Waals interactions. This is primarily due to scarcity of polar groups such as
609 hydroxyl and amino in asphalt, which limited availability of hydrogen atoms for
610 bonding (Fig. 9 (c) and (d)). Additionally, steric hindrance effects further impeded
611 formation of hydrogen bonds between asphalt polar groups and in aggregate surface O
612 atoms.

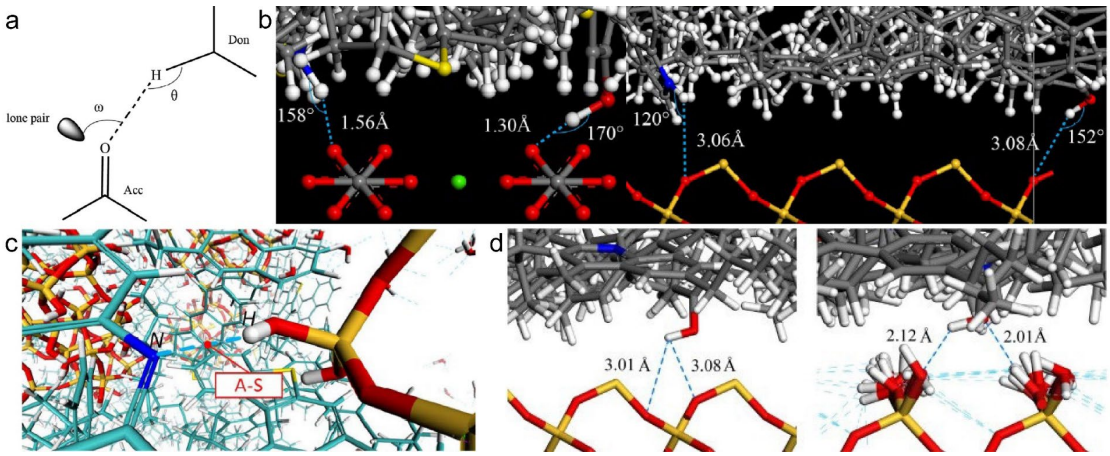

Fig. 9 Hydrogen bonds and distance of interface: (a) diagram of hydrogen bond; (b) hydrogen bonds between asphalt and SiO_2 and $CaCO_3$[94]; (c) hydrogen bonds between asphaltene and silica[107]; (d) distance between asphalt and un-hydroxylated and completely hydroxylated α-quartz-asphalt interface systems[108].

4. Impact of external factors on interfaces

4.1 Moisture environment

4.1.1 Weakening of binding and debonding energy

Moisture intrusion into asphalt-aggregate interfaces has an impact on molecular structure and component distribution of asphalt on aggregate surfaces. Although oxidative aging of asphalt affected interfacial adhesion energy with SiO_2 and $CaCO_3$ differently, the interfacial water consistently reduces adhesion energy, irrespective of type of aggregate, as shown in Fig. 10 (a). The resistance of asphalt mixtures to water damage depends on adhesion and debonding energy when water infiltrates interfaces[96, 109]. The introduction of a water film to interfacial models decreases potential energy compared to the sum of energies of original interfacial systems without water and isolated water layer without asphalt and aggregate. This indicates that water

630 films significantly reduce energy associated with direct interactions between asphalt
631 and aggregate. Moreover, within range of water film thickness considered in models,
632 thicker water films lead to more pronounced energy reduction[103]. The adsorbed water
633 molecules on weak alkaline aggregate surfaces impede distribution of asphalt
634 components near aggregate surfaces, thereby diminishing adhesion and altering
635 nanostructure of asphalt. Particularly, when free moisture infiltrates interfaces, the
636 adsorbed water interacts with free moisture, severely compromising moisture
637 susceptibility of asphalt mixture containing limestone and reducing its durability.
638 Similarly, water adsorbed onto surfaces of acidic aggregates negatively affects the
639 interfaces[110]. The abundance of hydroxyl groups on silica surfaces significantly
640 enhances hydrophilicity of surfaces and reduces its resistance to water damage[108]. In
641 asphalt-water-aggregate interfaces, water molecules induced morphological changes in
642 asphalt, which could be observed at various scales[111].

643 Hydrogen bonds play a crucial role in moisture damage at interfaces. The presence
644 of oxygen and hydrogen atoms in water molecules leads to formation of numerous
645 hydrogen bonds between water molecules, as well as between water and asphalt or
646 mineral[112]. Alongside hydrogen bonds, van der Waals and electrostatic also
647 contribute to interactions at interfaces, as illustrated in Fig 10 (b)-(d). Water molecules
648 readily adsorb on surfaces of aggregates, resulting in an increased spacing between
649 asphalt and aggregates. Consequently, as the interfacial distance expanded, the
650 interaction energy between asphalt and aggregates significantly decreases. When

651 interfaces are subjected to external stress in moisture environments, adhesion failure
652 tends to occur primarily within water layers due to comparatively weaker cohesion
653 between water molecules compared to asphalt molecules. The influence of hydrogen
654 bonds on debonding energy varied, as it increases for SiO_2 but decreases for
655 $CaCO_3$[113].

656 On calcite surfaces, the contact angle of water and asphalt were 13.8° and 87.2°.
657 The water droplet on un-hydroxylated α-quartz and completely hydroxylated α-quartz
658 surfaces were 104.7° and 34.5° (Fig. 11 (c)). This indicated that hydrogen bonds readily
659 formed between hydroxyl groups on silica surfaces and free water molecules,
660 facilitating water adsorption onto aggregate surfaces. In the presence of water at
661 interfaces, hydrogen bonds generate between hydroxyl groups on surfaces of silica and
662 water molecules are significantly stronger than attraction between aggregate surfaces
663 and asphalt molecules. Calcite surfaces exhibit a stronger affinity for water compared
664 to asphalt under same conditions. When gaps exist at interfaces, water adsorbs more
665 readily than asphalt onto calcite surfaces due to their differential affinities with
666 calcite[71]. The entry of water molecules leads to a reduction in interfacial directly
667 contacted zones, suggesting a trend for debonding. The distance of interface expands
668 although water molecules primarily distribute at edge of interfaces[73]. The contact
669 angle of water on asphalt surface is typically much larger than that on aggregate surface,
670 particularly at low temperatures, as shown in Fig. 11 (a)-(g). Asphalt was often
671 hydrophobic, facilitating adsorption of water molecules by aggregate interfaces, which

672 results in formation of a thin water film on aggregate surfaces. This film acted as a

673 barrier, impeding contact between asphalt molecules and aggregate interfaces.

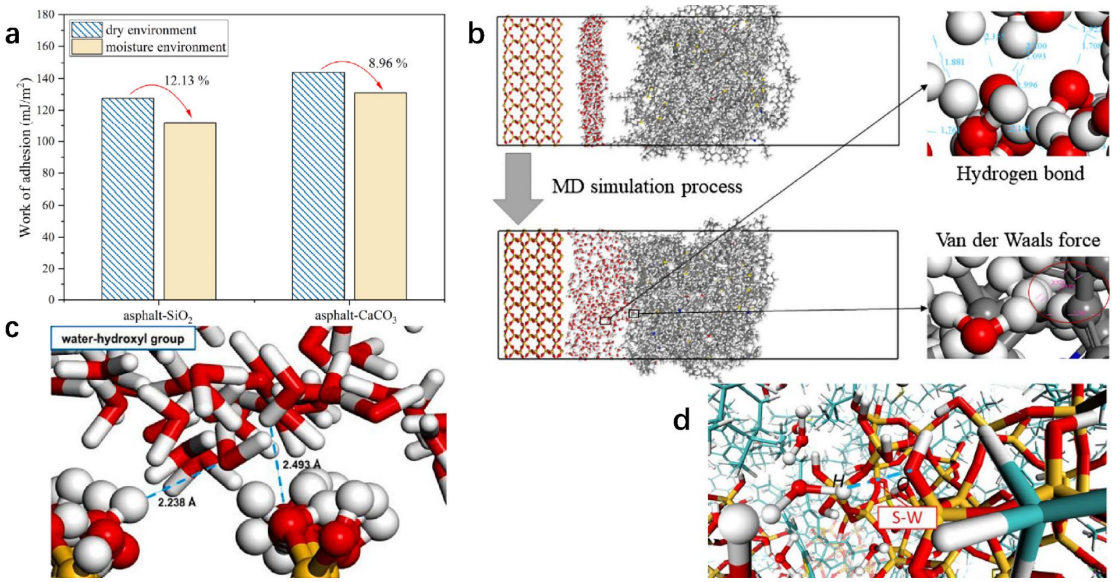

674

675 Fig. 10 Interfacial adhesion under moisture environments: (a) decrease of adhesion

676 work[71]; (b) interaction of interface[114]; (c) and (d)hydrogen bonds between water

677 and aggregate surface[115].

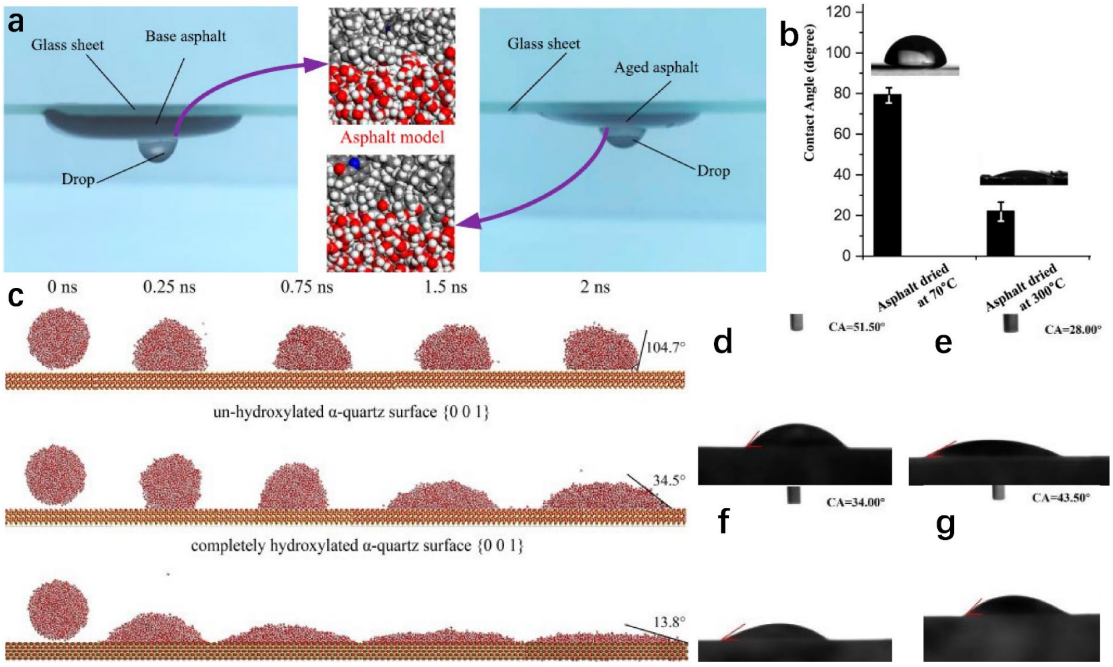

678

679 Fig. 11 Water contact angle: (a) water on asphalt surfaces[116]; (b) contact angles of

asphalts at 70 and 300 ℃[117]; (c) wetting process of water nano-droplets on α-quartz and calcite surfaces[108]; (d)-(g) contact angle of water with limestone, diorite, diabase, and steel slag[75].

4.1.2 Mobility of water molecules

The diffusion or mobility which estimated by MSD (Fig. 12 (a)) of moisture play a pivotal role in degradation of asphalt. The presence of water molecules significantly affects hydrogen bonds and cohesion within asphalt. The concentration of moisture has a notable impact on diffusion and structural arrangement of water molecules, particularly at low concentrations where a favorable dispersion of water molecules within asphalt promoted formation of hydrogen bonds with asphalt molecules (Fig. 12 (b)). Concurrently, moisture has potential to reduce intermolecular interaction among asphalt chains, potentially leading to stripping or cohesive failure of asphalt[107]. The diffusion path of moisture follows intricate 3-dimensional tortuous curves, and distribution of moisture is influenced by factors such as air voids and types of asphalt mixtures. Notably, the moisture diffusion is the highest in z-direction and has a high correlation with temperature, as shown in Fig. 12 (c)[118].

Enhanced diffusion of water molecules leads to increased moisture intrusion and larger interface gaps. Under moisture environments, adhesion of interfaces is compromised due to intrusion of moisture. $CaCO_3$ adheres with more asphalt, primarily attributed to intensified adsorption resulting from acid-base reactions[71]. The adsorption between asphalt and water molecules on mineral surfaces influences

susceptibility to moisture, indicating that aggregates rich in nepheline, chlorite, pyroxene, and olivine minerals tend to exhibit improved resistance to moisture damage, whereas aggregates with higher quartz, plagioclase, and calcite mineral content demonstrated the opposite trend[60]. The Diffusion coefficient of water molecules is more influenced by hydraulic pressure rather than humidity or aggregate type, highlighting a significant role of hydraulic pressure in moisture diffusion[119].

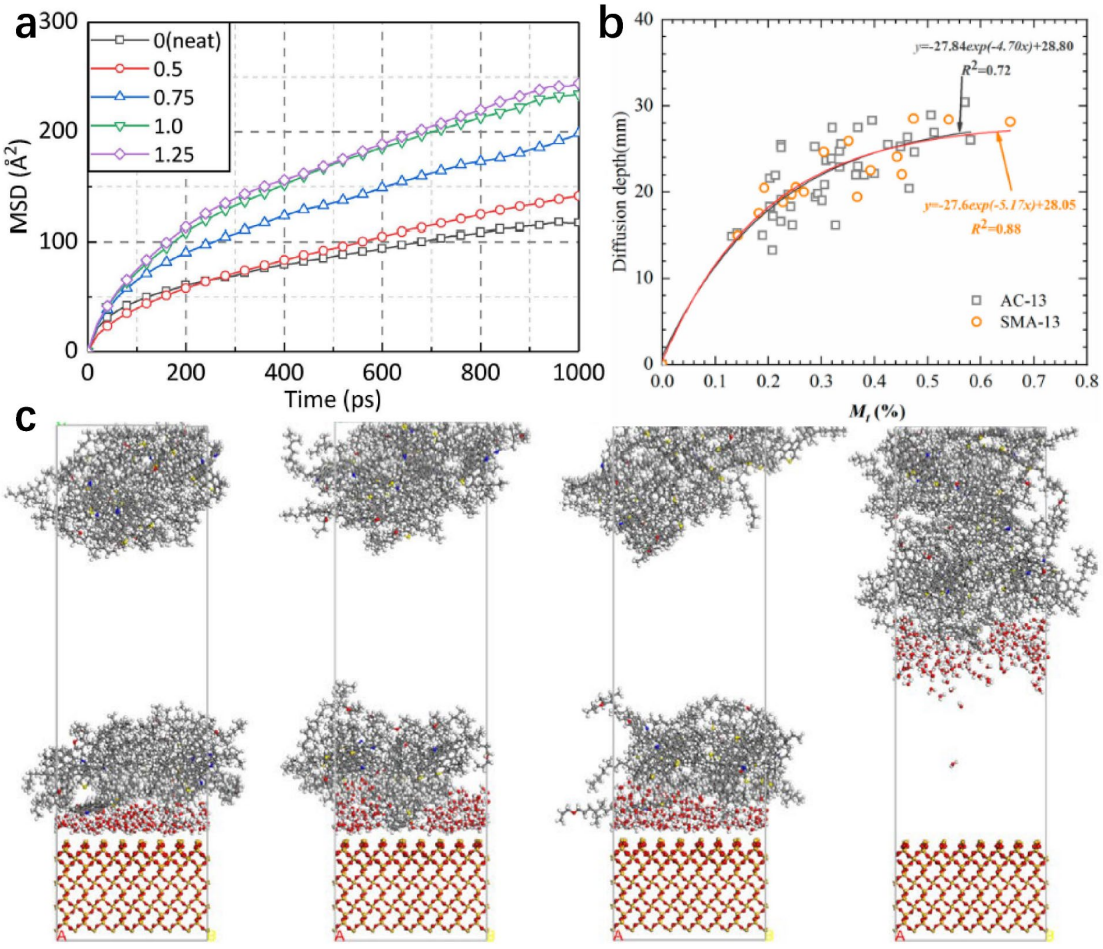

Fig. 12 Diffusion of water molecules in interface: (a) diffusion of water in asphalt[107]; (b) relationship between diffusion depth and moisture uptake[120]; (c) water in interface at 278.15, 298.15, 318.15, and 338.15 K[104].

4.1.3 Ionic solution erosion

Ionic solution models are employed to examine the erosion of seawater on asphalt-aggregate interfaces, as shown in Fig. 13[121-124]. Seawater composition is complex, with sodium ions (Na^+) and chloride ions (Cl^-) being predominant, while sulfate ions (SO_4^{2-}), magnesium ions (Mg^{2+}), and calcium ions (Ca^{2+}) exist in smaller amounts. Other microelement ions such as carbonate ions (CO_3^{2-}), heavy metal ions, and halide ions are present in trace quantities (Fig. 13 (b)). The erosion causes by chloride ions induced structural changes in asphalt film surfaces, leading to formation of a weak adhesion gradient zone. The concentration of chloride ions accelerated development of these unstable gradient zones over time. Consequently, water molecules easily infiltrate asphalt film and touch asphalt-aggregate interfaces through adsorption and diffusion, thereby weakening interfacial adhesion[125, 126]. During Cl^- erosion, resins exhibit high activity and readily adsorb onto silica surfaces. The distribution of asphaltenes, aromatics, and saturates are more uniform. The proximity of resin and aromatic molecules attract some aromatics to silica surface, causing a partial displacement of saturate and asphaltene molecules. Thus, the SARA components rearrange on silica surfaces. The interfacial adhesion is primarily influenced by resins and aromatics, with minor contributions from asphaltenes and saturates. The changes in spatial distribution of these components are associated with formation of adhesion gradient zones. Sea salt weakens aggregation of asphaltene molecules and altered their spatial distribution in interfacial zone, resulting in damage to original colloidal structure of asphalt and

accelerating interfacial failure. The diffusion of water molecules is impeded by saline/alkali solutes, with water molecules exhibiting slower diffusion rated in a saline environment. Additionally, salt enhanced hydrogen bonds between water and silica. Notably, interactions between calcite and solution are observed at interfaces, with salt and alkali promoting debonding effects. The alkali solution causes deeper moisture damage than saline solution. In comparison, SBS asphalt binder demonstrates higher water stability than virgin asphalt under these conditions[127].

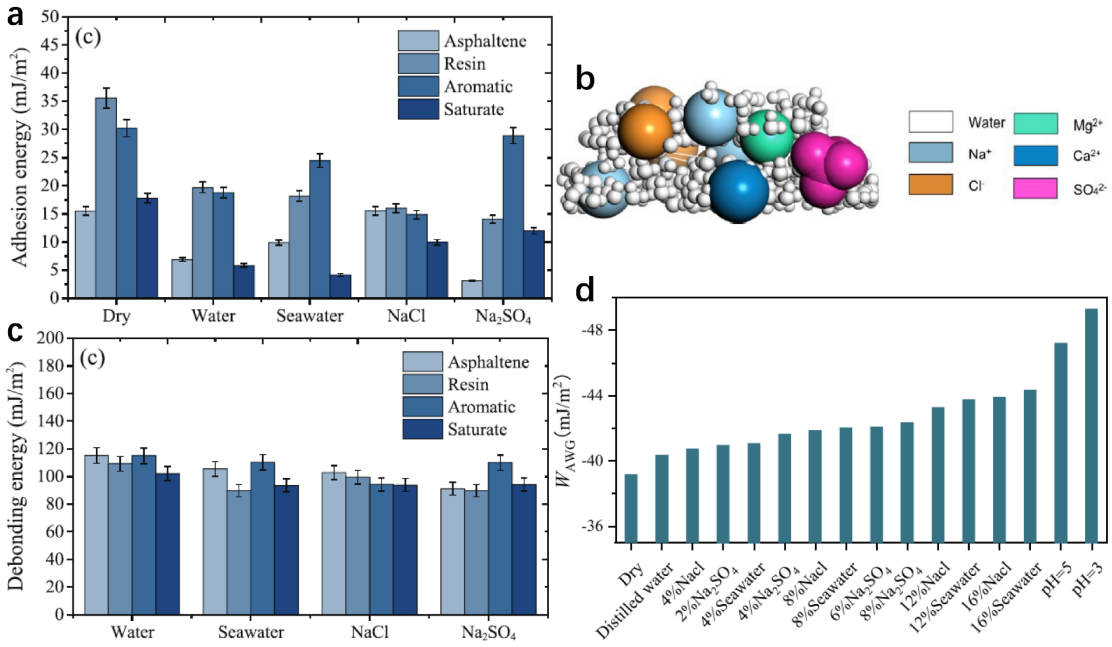

Fig. 13 Asphalt-solution-aggregate interface. (a) adhesion energy between asphalt and silica; (b) molecular model of seawater; (c) debonding energy between asphalt and silica[122]; (d) debonding work after salt and acid erosion environment[128].

4.2 Temperature variation

MD comparing virgin and aged binders reveal variations in characteristics at different temperatures[129]. As temperature rises, the asphalt undergoes a transition from a glass state to a liquid state, with most molecules becoming mobile and solid

747 fraction in colloid becoming negligible. Although temperature primarily affects asphalt
748 and water molecules rather than aggregate surfaces, it has a significant impact on their
749 behavior. Increased temperature promotes movement and collision of asphalt and water
750 molecules due to enhanced molecular mobility. Conversely, when temperature drops,
751 the solid components in asphalt increased, reducing molecular fluidity[130]. The
752 influence of temperature on interfacial adhesion failure is complex. Rising temperature
753 increases activation and interaction energy between asphalt and aggregates.
754 Macroscopic experiments confirm that asphalt soften at high temperatures and fill
755 micro voids between asphalt and aggregate due to its increased fluidity, leading to a
756 larger specific surface area. At molecular level, higher temperatures accelerate
757 movement of asphalt molecules, increasing probability of forming a stable distance
758 layer on aggregate surfaces and strengthening van der Waals forces between asphalt
759 and aggregates[70].

760 However, the cohesive energy of asphalt molecules increases with increasing of
761 temperature, leading to self-aggregation. Consequently, asphalt molecules tend to
762 gather away from aggregate layer. Under external stress, higher temperatures increase
763 likelihood of adhesion failure at interfaces due to self-aggregation. For example, the
764 presence of water at interfaces amplifies the effect of temperature on adhesive failure.
765 Moisture-induced degradation of adhesion is more pronounced at higher temperatures,
766 indicating an increased moisture sensitivity of asphalt binders. Elevated temperatures
767 enhanced activity and mobility of water molecules, intensifying their impact on

768 interface gaps. The accelerated movement of water molecules requires more space,
769 leading to continuous disruptions at asphalt-aggregate interfaces and causing asphalt to
770 displace from aggregates. In multi-cycling temperature conditions, the adhesion at
771 asphalt-quartz interfaces decreases, making them more susceptible to moisture damage
772 and cracking, as observed in high-low temperature cyclic tests[104]. This is because
773 the energy of interfaces undergoes a significant temperature increase and decrease, and
774 also undergoes a significant change. Due to drastic fluctuation of energy, the degree of
775 chaos in systems increases, and orderliness and stability of interfaces decrease, resulting
776 in separation of asphalt and aggregates. At low temperatures, the occurrence of micro
777 adhesion at asphalt-aggregate interfaces is predominantly influences by wetting effect
778 of light components on aggregate surfaces. However, the ability of aged light
779 components to sufficiently wet aggregate surfaces decrease, leading to reduced
780 microscopic adhesion at asphalt-aggregate interfaces. Among SARA components,
781 aromatics have the most significant impact on micro adhesion at low temperatures,
782 followed by saturates, while asphaltenes have the least effect[79]. Higher temperatures
783 facilitate faster self-aggregation between asphalt molecules, resulting in improved
784 efficiency. Furthermore, the presence of Fe_2O_3 in comparison to SiO_2 enhances
785 temperature sensitivity of asphalt and increases diffusion of molecules with rising
786 temperature. This enhancement is attributed to higher adhesion between Fe_2O_3 and
787 asphalt as well as superior thermal conductivity of Fe_2O_3, ultimately leading to
788 enhanced self-healing performance[131].

4.3 Improvement of adhesion by modifiers

Various polymer modifiers, such as styrene-butadiene-styrene (SBS), styrene butadiene rubber (SBR), polyurethane (PU) and polyphosphoric acid (PPA), are commonly incorporated into asphalt binders to look forward to improving performances of asphalt pavement. These modifiers serve multiple functions, including enhancing different properties of asphalt binders and fulfilling specific roles. The molecular interaction between modifier and virgin asphalt, resulting from both physical blending and chemical reactions, plays a vital role in determining microphase separation of modified asphalt[132]. Furthermore, the nature of this interaction is influenced by specific type of modified asphalt, aligning with experimental observations and demonstrating consistency with empirical findings (Fig. 14 (a))[133].

The natural rubber (NR) is selected as representative of crumb rubber (CR) due to its significant presence in tires in most previous studies[134]. It is a homopolymer resulting from polymerization of isoprene monomers, with varying degrees of polymerization ranging from tens to hundreds. The addition of NR in asphalt leads to an increase in electrostatic at interfaces, consequently enhancing adhesion between asphalt and aggregate. The different rubber contents change van der Waals forces but do not change electrostatics in adhesion (Fig. 14 (b))[99]. The adhesion is primarily governed by non-bonded interactions, indicating the absence of chemical bonding between NR and aggregates. Another representative CR, SBR, consisting of styrene, trans-1,4 butadiene, cis-1,4 butadiene, and 1,2-butadiene polymers, is also investigated.

The adhesion properties between limestone and CR asphalt are found to be more influenced by water compared to basalt[106, 135].

The CRs used in MD underwent a vulcanization process, during which sulfur crosslinks formed a stable three-dimensional network structure by cross-linking rubber chains. However, in CR modified asphalt, CR experiences a degradation reaction during preparation. This degradation process involves a desulfurization stage, where lower bond energy sulfur crosslinks are broken, and a depolymerization stage, where higher bond energy rubber chains are broken. These degradation behaviors of CR contribute to improved compatibility with asphalt, resulting in a significant increase in binding energy between rubber and asphalt. Consequently, a more stable molecular structure of CR modified asphalt binder is achieved[136]. The CR also exhibits the ability to adsorb asphalt molecules. Notably, the agglomeration of rubbers with aromatics/ saturates is more pronounced than that of asphaltenes with aromatics/ saturates. The agglomeration of rubbers-aromatics is also more clustered than that of rubbers-saturates. Additionally, the proportion of aromatics/ saturates in asphalt binder influences formation of a more clustered agglomeration structure between rubber and asphalt[137]. Interfacial interactions between rubber and asphalt have a potentially negative impact on cohesive strength, particularly in virgin binders compared to rubberized reclaimed asphalt pavement (RAP) binders. As shown in Fig. 14 (c), the trend and peak of overall RDF of two asphalts and three aggregates are basically similar, indicating that nonbond interactions between rubber/ asphalt and aggregates play an important role (Fig. 14 (d)),

because main components in rubber/ asphalt are saturated alkane segments and benzene rings. However, RAP incorporation in rubber binders predominantly disrupts homogeneity of binder colloid, while cohesive strength is significantly influenced by interfacial interactions[138].

SBS has been widely utilized in road asphalt engineering due to its remarkable modification capabilities in terms of high and low temperature performances, rheological properties, as well as its convenient preparation and cost-effectiveness. From a molecular structure perspective, SBS and rubber share similarities, and their effects on overall interface systems are comparable in MD. In general, rubbers possess longer molecular chains and heavier individual molecules compare to asphalt. Considering each rubber molecular contain multiple independent benzene rings and a lengthy main chain, the proportion of rubber molecules in modified asphalt systems is relatively small. Consequently, the influence of modifiers on entire systems was limited from standpoint of MD[114]. Both rubber and SBS contain numerous styrene structures along their molecular chains. These benzene ring structures, individually link to a main chain, readily interact with certain asphalt components containing benzene ring structures, particularly asphaltenes with island aromatic rings, through π-π stacking interactions between benzene rings. SBS can adsorb portions of asphalt molecules, thereby maintaining structural stability of asphalt binder which is confirmed laterally by SEM and FM (Fig. 14 (e) and (f)). Interactions between SBS and asphaltenes are also observed, facilitate by side chains of asphaltenes. Additionally, the π-π interactions

within condensed aromatic ring regions persist In Fig. 14 (g), the interaction between resins and SBS molecules primarily occur due to presence of aromatic ring regions. This is attributed to lower number of aromatic ring regions in resins, allowing for easier adjustment of their spatial conformation and facilitating the identification of binding sites with SBS molecules.

Besides, the substantial molecular segments of SBS or rubber in modified asphalt systems occupy a significant amount of space, leading to physical disruption of self-aggregation among polar molecules in asphalt. As a result, the cohesive energy between asphalt molecules is effectively reduced. This reduction in cohesive energy has potential to decrease likelihood of interfacial adhesion failure from a stress-strain failure perspective. Furthermore, the huge molecular weight of SBS or rubber themselves significantly contributes to calculation of interaction energy with aggregates. Longer chain segments result in stronger van der Waals forces between modifiers and aggregates, and movement of SBS or rubber molecules is relatively slower compared to other molecules in binder. Macroscopically, modifiers such as SBS and CNTs formed a three-dimensional network structure within asphalt, thereby enhancing overall stability of modified asphalt and its interaction energy with aggregates[139].

The interactions between SBS and asphaltenes occur through branch chains, leading to attraction of some asphaltene aggregations to SBS. Saturates molecules surrounded SBS molecules, while resins/ aromatics molecules, with greater spatial flexibility and adjustability, tend to adsorb around SBS[140]. Comparatively, the

873 compatibility is higher between nonpolar components and SBS, but lower between
874 polar components and SBS. To achieve high-performances, it is recommended to blend
875 SBS with asphalt containing more aromatics and less asphaltenes, enhancing interfacial
876 properties and compatibility[37]. The addition of SBS significantly improves moisture
877 resistance of modified binder compared to unmodified binder, as evidenced by
878 debonding work. The adhesion between SBS and SiO_2 is mainly attributed to Van der
879 Waals[141]. Moreover, the interfacial heat transport capability is greatly enhanced with
880 incorporation of SBS molecules[142].

881 The molecular properties of other polymer-modified asphalts, such as PPA and PU,
882 also have been investigated in previous studies, although they are less commonly used
883 in road modifications compared to CR and SBS[143]. However, when considering these
884 modifiers at a molecular level, their interaction energy with aggregates might be higher.
885 This is attributed to the presence of numerous polar functional groups in these polymer
886 molecules, such as -OH, -P=O, and -C-O-C-. These functional groups form multiple
887 hydrogen bonds with aggregates, thereby increasing overall interaction energy[93]. PU
888 molecules possess heteroatoms such as nitrogen and oxygen, as well as polar functional
889 groups like ester and carbonyl groups, along with benzene rings. These structures
890 impart higher polarity to polyurethane compared to ordinary asphalt molecules.
891 Consequently, the addition of PU or PPA as modifiers in asphalt leads to an increase in
892 overall polarity of modified asphalt systems[144-146].

893 Carbon materials, such as graphene and CNTs, have attracted considerable

attention for their remarkable performance when incorporate into asphalt. Besides abundant continuously and widely distributed benzene rings, these carbon materials actually exhibit excellent conductivity. When interacting with aggregates, particularly those composed of ions, the interaction encompasses not only van der Waals but also significant electrostatic forces. The addition of CNTs to asphalt improves adhesion at asphalt-aggregate interfaces and enhances adsorption capability of asphalt on alkaline aggregates through electrostatic effects[147]. CNTs, possessing numerous active adsorption sites in asphalt, demonstrate a strong affinity for abundant Ca^{2+} and Mg^{2+} ions present in calcite, thereby enhancing electrostatic interactions between asphalt and alkaline minerals. It is attributed to formation of a highly interconnected 3D network between ionic sites and asphalt, greatly enhancing asphalt elasticity. Modifiers with benzene rings interact with the aromatic rings of asphalt molecules, limiting their free dispersion on asphalt surfaces[148]. When graphene or CNTs are uniformly dispersed in asphalt, they form a 3D network structure. The network structure hinders relative movement of asphalt molecules, enhances deformation resistance of asphalt, and ensures that, under high-temperature or stress tensile conditions. It also restricts significant molecular displacement, effectively prevents rapid separation of asphalt molecules from aggregate layer and interfacial adhesion failure. Furthermore, the CNT network structure impedes penetration of oxygen atoms and water molecules into asphalt[149]. By limiting access of oxygen and water, the 3D network structure reduces negative impact of aging and interface separation of asphalt molecules, thereby

mitigating occurrence of interfacial failure.

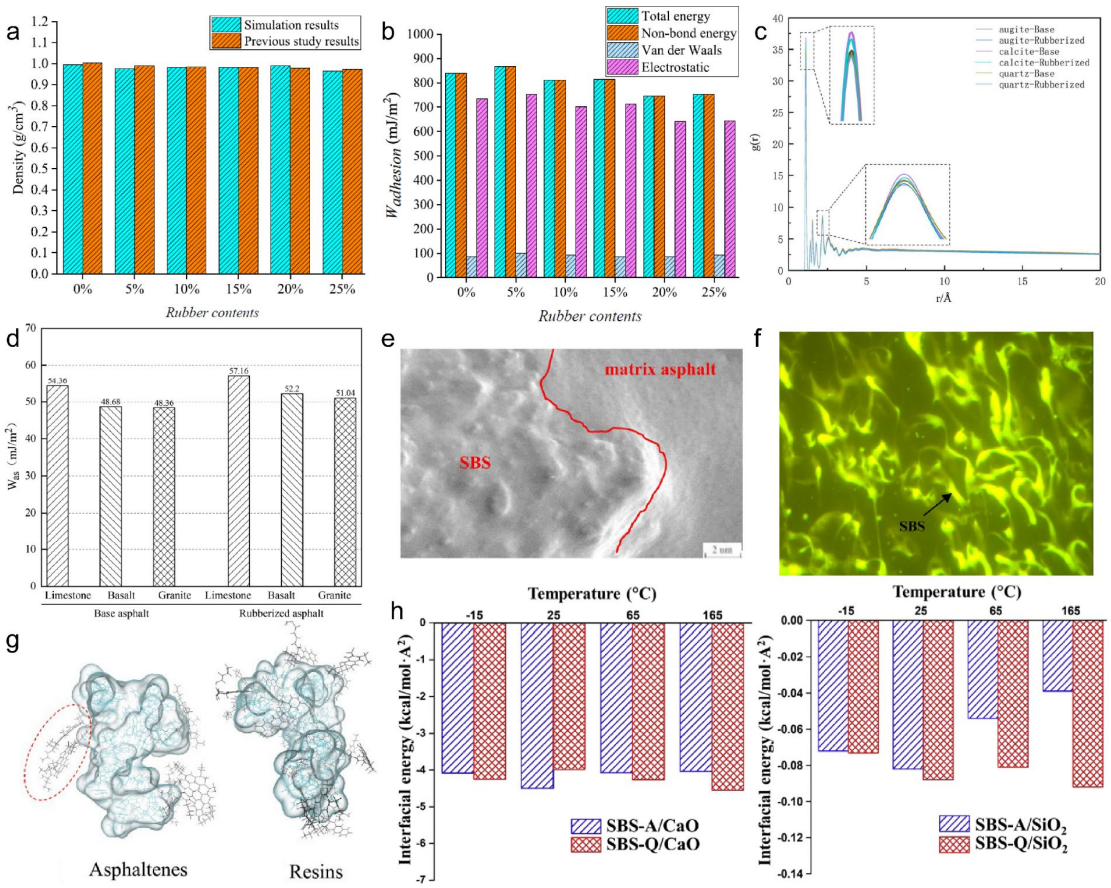

Fig. 14 Properties of polymer modified asphalt and aggregate interfaces: (a) density of rubber asphalt between simulation and test results; (b) adhesion between quartz and rubber asphalt[99]; (d) RDF of different aggregate with rubber asphalt; adhesion work of different aggregates to rubber asphalt[150]; (e) and (f) SEM and FM images of SBS modified asphalt[23]; (g) asphaltenes and resins distribution within 2.5 Å of SBS[140]; (h) interfacial energy values of SBS asphalt-aggregate interface[151].

4.4 Aging and regeneration of interfaces

4.4.1 Aging of asphalt

During service life of asphalt, various factors such as high temperature, light, moisture, oxygen, solar radiation, and ultraviolet radiation contribute to its aging

process. Aging leads to a transformation in inner structure of asphalt, transitioning from a soft and fluid state to a rigid and stiff state. As shown in Fig. 15 (a) and (b), the surface morphology of asphalt undergoes significant changes with an evident increase in surface roughness occurring as aging degree deepens. AFM images reveal augmented number, area, and height of bee-structures on asphalt surface after aging. This change is attributed to component transformation of asphalt during aging, particularly the increase in polar heavy components such as asphaltenes, which promotes formation of bee-structure. SEM images elucidate the reason behind increased surface roughness of aged asphalt at micro scale. The increase in polar components during aging facilitates aggregation among these constituents, leading to separation of light and heavy components and subsequent formation of microcracks on surfaces. These microcracks contribute to interfacial failure between asphalt and aggregates. During aging, the light components evaporate or transform to heavy components, wherein aromatics convert into asphaltenes or polar resins due to generation of oxygen-containing functional groups (S=O and C=O which could be seen in FTIR as shown in Fig. 15 (c)) in asphalt molecules[152]. In initial stage of aging, hydrogen abstraction on asphaltenes triggers two sub-reactions. First, aromatization of cycloalkanes occurs, enhancing dispersion in asphaltene molecules through increased π-π interactions. Second, oxygen-containing groups generate, amplifying electrostatic interactions in asphaltene molecules by enhancing their polarity. Consequently, molecular agglomeration within aged asphalt intensifies and increases modulus and adhesive force. As aging progresses further, some

948 small molecules and side chains detach from asphaltenes, leading to a reduction in size,
949 aromaticity, and polarity of molecules[89]. S=O groups form earlier than C=O groups.
950 Higher temperatures accelerate oxidative aging, with temperature exerting a greater
951 influence on generation of C=O groups compared to S=O groups. Initially, hydroxyl
952 groups on aromatic rings undergo oxidation to form C=O groups, followed by oxidation
953 on benzyl carbons. But some benzyl carbons may not undergo the transformation into
954 C=O groups. Hydroxyl groups are observed as intermediate oxidation products prior to
955 formation of C=O groups[153].

956 The interfacial adhesion and diffusion of asphalt on mineral surfaces rapidly
957 decline following aging. This decline diminishes further with aging deepening.
958 Saturates and aromatics in aged asphalt are insufficient to adequately wet mineral
959 surfaces, resulting in a decrease in adhesion[79, 154]. Aging benefits adhesion of dry
960 asphalt-calcite interfaces by enhancing electrostatic interactions due to increased
961 molecular polarity. Aging functional groups C=O and S=O actively participate in
962 formation of hydrogen bonds, increasing the adhesion strength of interface (Fig. 15 (d)).
963 In wet conditions, the ratio of residual adhesion to that in dry conditions indicates
964 consistently higher moisture susceptibility after aging, suggesting an increased
965 propensity for moisture damage in asphalt pavement[90, 155]. After aging, the
966 interaction energies between asphalt and water molecules increase, primarily due to
967 formation of more and stronger hydrogen bonds[156].

968 In general, the binding energies of aged asphalt to aggregates is greater compared

969 to unaged asphalt (Fig. 15 (e)). This increase is attributed to presence of polar molecules,
970 which enhances interaction energy through van der Waals, electrostatic, and hydrogen
971 bonds effects. The polar functional groups contribute to adhesion strength of asphalt
972 and aggregates[157]. However, the energy of aged asphalt itself is also greater than that
973 of unaged asphalt, primarily due to higher polarity. In practical applications of asphalt
974 pavement, adhesion failure typically occurs under stress. The internal interactions
975 present in aged asphalt make it more susceptible to adhesive failure rather than cohesive
976 failure, despite its stronger bonding with aggregate surfaces. This also explains why
977 even though aging asphalt produces stronger bonding with aggregate surfaces, it is more
978 prone to spalling behavior.

979 The mechanism evaluation of asphalt aging behavior on MD is summarized,
980 including macroscopic physical properties, mesoscopic chemical compositions,
981 microscale morphologies, and nanoscale molecular structures[158]. The asphalt aging
982 leads to changes in molecular composition and structure, leading to an increase in
983 overall size and density of lattice cells and internal energies. From molecular-level
984 perspective, oxidative aging leads to an increase in intermolecular cohesive strength
985 and a reduction in diffusion ability[159]. The increase of CED and FFV result in asphalt
986 hardening and stiffing due to formation of polar functional groups, which products
987 strengthen intermolecular bonding(Fig. 15 (f) and (g))[160].

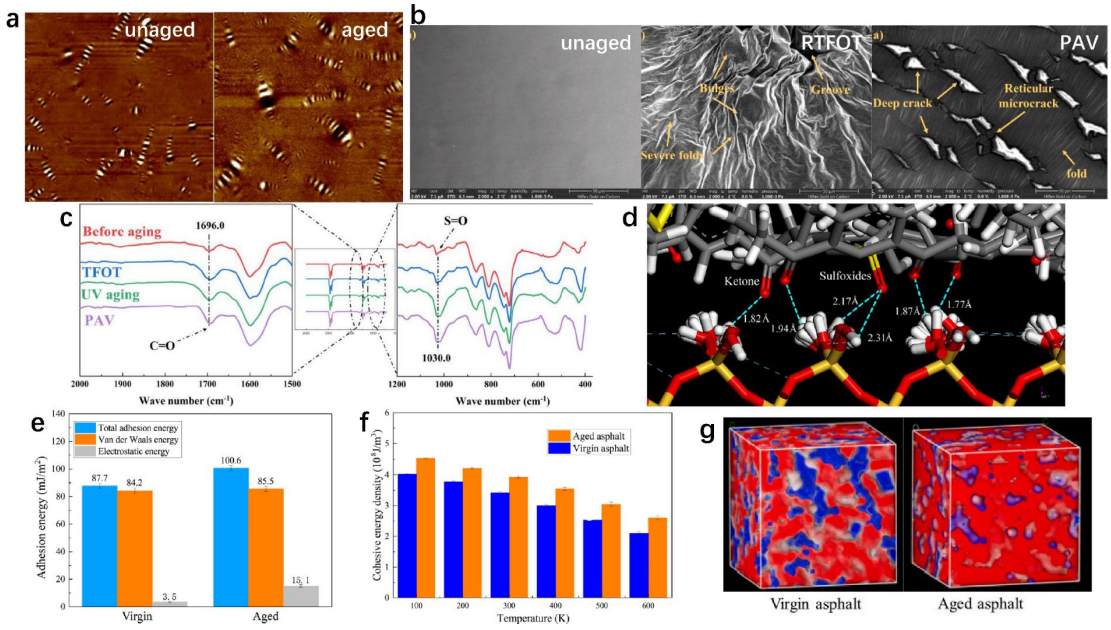

Fig. 15 Effect of aging on asphalt and interface: (a) AFM diagram of unaged and aged asphalt[161]; (b) SME of different aging degrees[162]; (c) FTIR of different aging degrees[163]; (d) interaction between functional groups in aged asphalt and aggregate; (e) adhesion between asphalt and SiO_2; (f) CED of unaged and aged asphalt[48]; (g) free volume distribution of unaged and aged asphalt[164].

4.4.2 Rejuvenators for performance recovery

RAP utilizes various rejuvenators to restore physicochemical and mechanical properties of aged asphalt. Due to excellent environmental and economic benefits, RAP becomes an effective solution to save cost of maintenance and reconstruction in pavement engineering[165, 166]. Generally, rejuvenators help to improve diffusion behaviors of aged asphalt binder. Notably, naphthene aromatics of rejuvenators exhibit the highest diffusion coefficient due to their benzene ring structure, while small and light molecules possess inherent advantages in terms of diffusion[167]. Rejuvenators influence structures and distributions of asphalt molecules, leading to rejuvenated

configurations[91].

The waste cooking oil (WCO), a viscous greasy substance resulting from frying processes, has gained significant attention as an additive in aged asphalt binders to restore their performance[168]. The waste vegetable oil (WVO), such as soybean, palm, corn, peanut, rape, and sunflower [169, 170], alongside animal greases like lard and fish oil, also are usually used rejuvenators if they are waste[171]. The primary constituents of WCO consist of saturated and aromatic fractions, referred to as light components. Comprised mainly of C, H, and O, with minor traces of S, N, or P, WCO exhibits a slightly higher O content compared to asphalt due to oxidation during producing at high temperatures. The rejuvenators rich in light components contribute to rebalancing ratio between light and heavy components and mitigating impact of polar functional groups in heavy components. WCO, predominantly composes of triglycerides containing various fatty acids in their side chains, facilitates transformation of large asphaltene aggregated into smaller structures. The alteration in distribution of asphaltenes increases in mobility of asphalt during self-healing process. By enhancing mobility of asphalt, WCO elevates flow and fatigue resistance of asphalt, thereby contributing to its self-healing efficiency[172]. Additionally, the addition of WCO disrupts original agglomeration by forming strong O-H bonds between negatively charged O atom in ester group and positively charged H atoms in molecules[92]. Furthermore, WCO restores molecular structure of aged asphalt, attenuating self-aggregation of asphaltenes, and modifying asphalt-aggregate interfaces,

thereby improving interfacial adhesion[173]. Waste engine oil (WEO), characterizes by a molecular structure resembling that of WCO with numerous lightweight molecules, effectively decreases density and cohesive energy of aged asphalt, promotes increased flow diffusion and flexibility[174]. The waste oil rejuvenators can not only alleviate consumption of energy and resources to promise economic benefits but also eliminate potential hazards to food and environment safety. The first essential in MD of rejuvenator modified asphalt binder is the construction of various rejuvenators. It is worth noting that whether it is WCO, WEO, or some other rejuvenators, they are all complex mixtures. The components in these organic mixtures are difficult to characterize all specific molecules, so in MD studies, researchers have adopted representative molecules from them. In some different studies, the number of hydrocarbons in rejuvenator molecules will roughly fluctuate by one to two. Some representative models of rejuvenator molecules are shown in Fig. 16.

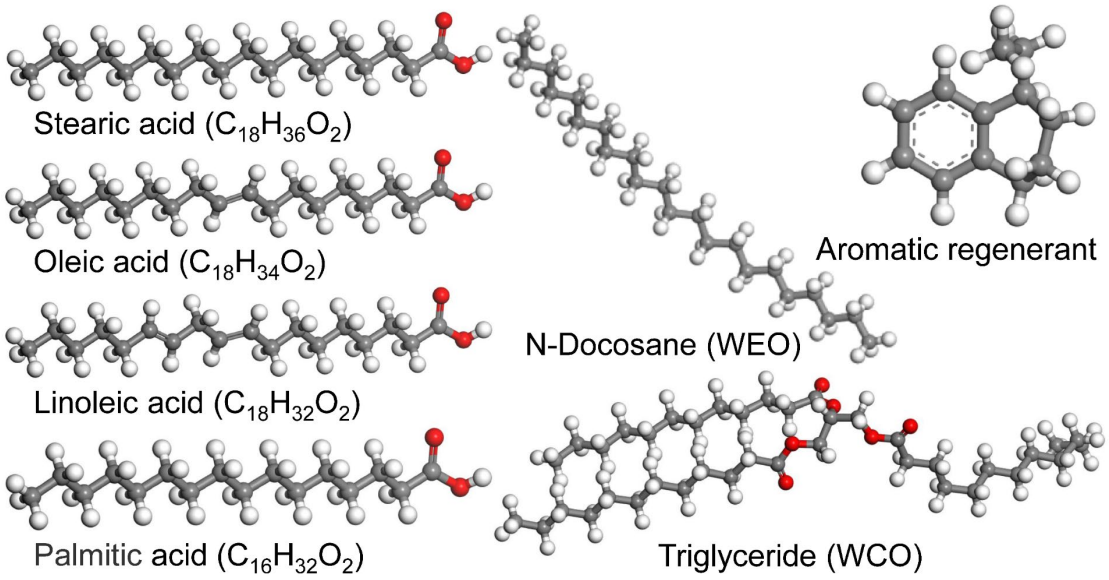

Fig. 16 Stearic acid, oleic acid, linoleic acid, and palmitic acid were widely present in

1039 animal and vegetable fats and were the main components of WCO; $C_{12}H_{16}$ was the
1040 common model of aromatic regenerant; N-Docosane (C22H46) was the main
1041 component of WEO; Triglyceride also was a representative model of WCO[175, 176].
1042 The characteristics of rejuvenators possess not only a softening effect but also
1043 ability to effectively interact with oxidized asphaltenes, leading to their
1044 deagglomeration[175]. Evaluating compatibility between rejuvenators and asphalt
1045 binders relies on two critical indicators: CED and solubility (δ) (Fig. 17 (a)). The C=O
1046 and S=O groups enhance intermolecular force and cohesive energy in aged asphalt,
1047 resulting in increased stiffness and reduced compatibility as aging deepens[45].
1048 Variations in compatibility are observed among different rejuvenators, all oil-based
1049 rejuvenators positively contribute to performance improvement. The molecular
1050 structures of most waste oils comprise numerous long straight saturated segments and
1051 ester groups. Benzene rings in the long straight chain segments prevent parallel
1052 adsorption of bonds with polar functional groups, especially continuous benzene ring
1053 structures found in asphaltenes and resins. Additionally, saturated structures of oil
1054 molecules allow for easy insertion of these segments between parallel-oriented polar
1055 molecules containing benzene rings, disrupting their bonding and diluting
1056 concentration of benzene ring bonding in aged asphalt. As shown in Fig. 17 (c) and (d),
1057 small WCO molecules surround asphaltenes and prevent aggregation. WCO molecules
1058 improve distribution of asphaltene, enhances compatibility in colloids, and restores
1059 colloidal structure in binder, thereby improving rheological properties of binder[177-

179].

However, the influence of oil on adhesion of interface is not singular (Fig. 17 (e)-(h)). Various influencing parameters and diverse effects of rejuvenators on aged asphalt contribute to altered characteristics of interfaces. Waste oil, containing ester and terminal carboxyl groups, can form strong adsorption bonds with aggregate surfaces through van der Waals and electrostatic forces. The interaction energy between oil rejuvenators and aggregate often surpasses that of certain asphalt molecules, with preferential adsorption occurring on oxygen-functional group-rich side. The rejuvenation effect of WCO is evident in modulation of interfacial adhesion, where it enhances van der Waals with SiO_2 and electrostatic with $CaCO_3$, restoring adhesion work by modifying structure of aged asphalt molecules and establishing adhesion to aggregate[180]. Favorable temperature and permeation time facilitate penetration of bio-oil into aged asphalt[181]. The light components of oil rejuvenators improve flowability of overall structure of aged asphalt, thereby reducing its cohesive energy and total energy.

Concerning nanostructure of asphalt, the colloidal structure is partly restored, despite rejuvenators assisting in mitigating self-aggregation of asphaltenes. The rejuvenators enhance moisture damage resistance of aged asphalt, exhibiting improved adhesion with Al_2O_3 compared to SiO_2[182]. Rejuvenators also decrease debonding work between aged asphalt and aggregates, significantly increasing water stability and reducing moisture-induced interfacial adhesion deterioration. For most oil rejuvenators,

1081 they are hydrophobic molecules. When water molecules in interface gaps are squeezed
1082 by rejuvenator molecules, there is a greater probability that they would escape from
1083 interface gaps, thereby reducing moisture content in humid environments and reducing
1084 peeling energy of interfaces. WCO modifies structures of asphalt molecules and
1085 adhesion work at interfaces. WCO molecules exhibit a hydrophilic nature that allow
1086 water to penetrate asphalt, potentially compromising interfacial adhesion, while more
1087 likely to cause water-induced interfacial adhesion deterioration. Conversely, water
1088 penetration into reclaimed asphalt with WEO is hindered, but once inside, aromatic ring
1089 structures with hydrophobic properties facilitate water diffusion into asphalt-aggregate
1090 interfaces[183].

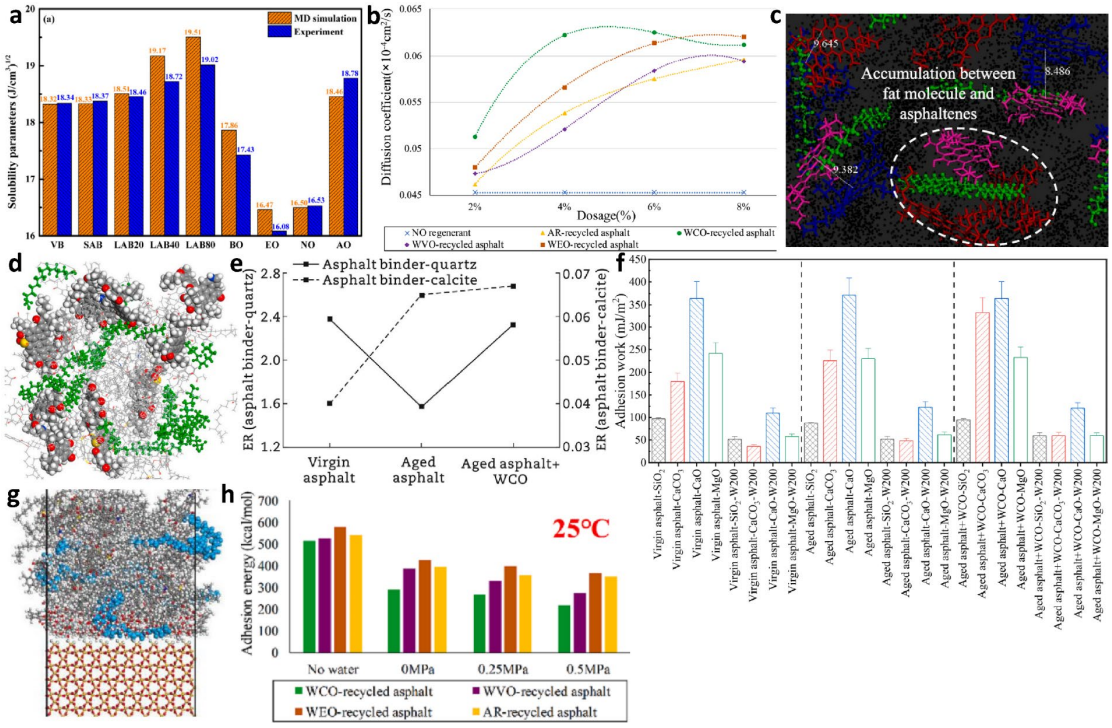

1091

1092 Fig. 17 Interaction of interfacial properties adding rejuvenators: (a) solubility parameter
1093 of rejuvenators, unaged and aged asphalt[45]; (b) diffusion coefficients of different
1094 rejuvenated asphalt; (c) stacking morphology in asphalt after adding regenerant[164];

(d) alignment of WCO and asphaltene molecules[184]; (e) energy ratios of asphalt-quartz and asphalt-calcite interfaces[173]; (f) adhesion work of virgin or aged asphalt-mineral interfaces under dry and wet conditions with or without rejuvenators; (g) WCO rejuvenated asphalt-water-quartz interface[180]; (h) adhesion energy of recycled asphalt-aggregate interface[183];

5. Conclusions and recommendations

5.1 Main conclusions

This review summarizes developments and current understanding of asphalt-aggregate interfaces under different conditions. Valuable insights into asphalt-aggregate interface effects are gleaned from MD modeling and simulations, coupled with remarkable strides in experimental techniques. Our focus remains on the adhesion between asphalt and aggregate, offering direction for the systematic design of high-performance asphalt mixtures with enhanced properties. Furthermore, we highlight MD as an influential tool that provides structural and dynamical information including adhesion/ cohesion of interface, asphalt molecules aggregation (shape, size, and distance), interfacial morphologies, water/ oxygen diffusion/ distribution, and influence of various molecular features (type of aggregates, compositions of asphalt, aging state of asphalt, temperature/ pressure conditions, dry/ moisture environments, different modifiers/ rejuvenators added to asphalt binder) on structural and dynamical properties.

MD simulation methods provides the technical basis for understanding interfacial properties between asphalt and aggregate. The advancements in software and databases

have afforded researchers a comprehensive way to engage in computational explorations on asphalt-aggregate interfaces that complement their experimental efforts. MD techniques have offered crucial structural insights essential for interpretation and validation of experiments. The hitherto unexplored spatial and temporal dimensions of adhesion between asphalt and aggregate have become accessible through computational simulations. MD provides a unique insight, presenting an accurate depiction of visible structure and dynamic status at molecular-level scale where asphalt interacts with aggregates. This enables the characterization of physicochemical and mechanical properties, giving new methods and techniques for establishment of novel theory of asphalt-aggregate interfacial adhesion.

The developments of MD allow applications to most asphalt-aggregate interface systems. These applications are plural and concern interfacial properties (adhesion, cohesion, binding, debonding, and aggregation), characteristics of asphalt and aggregates, and update iteration of modeling. In particular, MD is well suited to investigate interfacial properties of asphalt-aggregate interfaces, in which asphalt-aggregate interactions play an important role. Understanding the fundamental correlations among multiscale MD of asphalt, aggregates, and environments might pave the way to design and improve high-performance asphalt pavements. As repeatedly highlight, the combination of computational and experimental strategies offers an efficient way to explore for adhesion/ adsorption mechanism of asphalt-aggregate interfaces. Conclusively, the motivation for researchers to advance remains develop a

standardized modeling and simulation method for asphalt-aggregate interfaces, especially considering effects of multi interactions, different external conditions, various elements, differential forcefields.

5.2 Recommendations for future works

Nonetheless, MD simulations on asphalt-aggregate interfaces currently encounter some shortcomings, which can be categorized into three primary domains: (1) limitations related to accuracy of computational interface models used to represent asphalt-aggregate systems; (2) shortcomings due to computational techniques employ to simulate interfacial events; (3) constrictions because of relying on progress in physical and chemical analysis methods.

(1) In an ideal world, the MD will be the perfect tool of design and estimate of road asphalt materials. Unfortunately, although considering a large amount of factors, there is still a huge gap between artificial simulation data and real experimental results. As this will be existing circumstances for next several years, researchers are forced to focus their efforts on improving interfacial models, forcefields, parameters, and calculation methods to be close real experiments. This is a fundamental issue that affects MD of asphalt or aggregates materials as a whole.

(2) The limitations of simulations presently employed to investigate interfacial properties are lacking of a sufficiently large system, long time, and comprehensive reaction representations. The scale problems, including time- and space-scale, limit this approach to some simple processes without phase change, region change, and long

continuous processes, typically a little distant from realistic asphalt-aggregate interfaces. To a complex model system, the requirement of strong and high speed calculation capacity is necessary. At the moment, simulations of interfacial interactions of asphalt and aggregates are restricted to small systems (10^3 to 10^5 atoms), most often under idealized conditions. In the future, the MD of asphalt science and engineering must be considered at millimeter-scale and second-scale rather than nanometer-scale and nanosecond-scale. At the same time, the number of atoms, molecules, bonds, and energies that need to be calculated may reach several hundred million levels. However, nowadays, these techniques are computationally expensive considering time and equipment. The development of efficient calculation methods of a huge number of atoms and molecules is one of the urgent issues to be solved.

(3) It is hard to consider defects of aggregates, hetero-particles of asphalt, special molecules in interfaces, and different crystallization of aggregates. Indeed, non-uniformity and instability seem to be ubiquitous in many asphalt-aggregate interfaces. Non-uniformity and instability are also often associated with the instinct nature of asphalt and aggregate materials, but possibly due to the inherent difficulties in simulation. These are crucial factors that consistently influence measurements of adhesion performance on asphalt and, as such, should be integrated into asphalt-aggregate interfaces simulations as well. Much of future efforts must be dedicated to (i) enabling microscopic morphology observation of contact region of asphalt-aggregate interfaces, (ii) obtaining specific chemical compositions of asphalt and aggregates

based on chemical experiments, and (iii) creating a huge database unified experimental results and simulation data.

CRediT authorship contribution statement

Yujie Tang: Writing – original draft, Investigation, Methodology. **Zhen Fu:** Supervision, Validation. **Guido Raos:** Methodology, Writing - review & editing. **Feng Ma:** Supervision, Methodology. **Peng Zhao:** Writing - review & editing. **Yingjie Hou:** Writing - review & editing.

Declaration of Competing Interest

The authors declare that they have no known competing financial interests or personal relationships that could have appeared to influence the work reported in this paper.

Acknowledgments

This work was supported by National Key Research and Development Program of China (No. 2021YFB2601000) and Shaanxi Science and Technology Project (No. 2022KW-37).

Reference

[1] P. Wang, F. Zhai, Z.-j. Dong, L.-z. Wang, J.-p. Liao, G.-r. Li, Micromorphology of Asphalt Modified by Polymer and Carbon Nanotubes through Molecular Dynamics Simulation and Experiments: Role of Strengthened Interfacial Interactions, Energy & Fuels 32(2) (2018) 1179-1187.

[2] C. Siyu, L. Xiyin, L. Haoyuan, Y. Jiangmiao, C. Fuda, Z. Yang, M. Tao, H. Xiaoming,

A state-of-the-art review of asphalt pavement surface texture and its measurement techniques, Journal of Road Engineering 2(2) (2022) 156-180.

[3] F. Guo, J. Pei, J. Zhang, B. Xue, G. Sun, R. Li, Study on the adhesion property between asphalt binder and aggregate: A state-of-the-art review, Construction and Building Materials 256 (2020) 119474.

[4] Q. Jiang, W. Liu, S. Wu, Analysis on factors affecting moisture stability of steel slag asphalt concrete using grey correlation method, Journal of Cleaner Production 397 (2023) 136490.

[5] X. Chen, W. Wen, J. Zhou, X. Zhou, Y. Ning, Z.M. Liang, Zhenyu, Research on the Interaction Capability and Microscopic Interfacial Mechanism between Asphalt-Binder and Steel Slag Aggregate-Filler, Coatings 12(12) (2022) 1871.

[6] M. Mazumder, R. Ahmed, A.W. Ali, S.-J. Lee, SEM and ESEM techniques used for analysis of asphalt binder and mixture: A state of the art review, Construction and Building Materials 186 (2018) 313-329.

[7] X. Yao, H. Xu, T. Xu, Void distribution, interfacial adhesion and anti-cracking mechanisms of cold recycled asphalt mixture based on AFM and X-ray CT, Applied Surface Science 606 (2022) 155012.

[8] X. Wang, J. Liu, Z. Wang, H. Jing, B. Yang, Investigations on Adhesion Characteristics between High-Content Rubberized Asphalt and Aggregates, Polymers 14(24) (2022) 5474.

[9] Y. Hou, J. Li, X. Ji, H. Zou, C. Wang, X. Fang, Moisture Damage of Asphalt Based

on Adhesion, Microsurface Energy, and Nanosurface Roughness, Journal of Materials in Civil Engineering 34(10) (2022) 04022249.

[10] F. Noé, A. Tkatchenko, K.-R. Müller, C. Clementi, Machine Learning for Molecular Simulation, Annual Review of Physical Chemistry 71(1) (2020) 361-390.

[11] A. Glielmo, B.E. Husic, A. Rodriguez, C. Clementi, F. Noé, A. Laio, Unsupervised Learning Methods for Molecular Simulation Data, Chemical Reviews 121(16) (2021) 9722-9758.

[12] G. Raos, B. Zappone, Polymer Adhesion: Seeking New Solutions for an Old Problem, Macromolecules 54(23) (2021) 10617-10644.

[13] A. David, M. Pasquini, U. Tartaglino, G. Raos, A Coarse-Grained Force Field for Silica-Polybutadiene Interfaces and Nanocomposites, Polymers (Basel) 12(7) (2020) 1484.

[14] D. Bedrov, J.-P. Piquemal, O. Borodin, A.D. Mackerell, B. Roux, C. Schröder, Molecular Dynamics Simulations of Ionic Liquids and Electrolytes Using Polarizable Force Fields, Chemical Reviews 119(13) (2019) 7940-7995.

[15] G.C. Sosso, J. Chen, S.J. Cox, M. Fitzner, P. Pedevilla, A. Zen, A. Michaelides, Crystal Nucleation in Liquids: Open Questions and Future Challenges in Molecular Dynamics Simulations, Chemical Reviews 116(12) (2016) 7078-7116.

[16] S. Feng, S. Park, Y.K. Choi, W. Im, CHARMM-GUI Membrane Builder: Past, Current, and Future Developments and Applications, Journal of Chemical Theory

and Computation 19(8) (2023) 2161-2185.

[17] S. Sinha, C. Pindi, M. Ahsan, P.R. Arantes, G. Palermo, Machines on Genes through the Computational Microscope, Journal of Chemical Theory and Computation 19(7) (2023) 1945-1964.

[18] S. Safaeian Laein, I. Katouzian, M.R. Mozafari, A. Farnudiyan-Habibi, Z. Akbarbaglu, M.R. Shadan, K. Sarabandi, Biological and thermodynamic stabilization of lipid-based delivery systems through natural biopolymers; controlled release and molecular dynamics simulations, Critical Reviews in Food Science and Nutrition 2191281 (2023) 20.

[19] M. Ahmadi, E. Aliabadian, B. Liu, X. Lei, P. Khalilpoorkordi, Q. Hou, Y. Wang, Z. Chen, Comprehensive review of the interfacial behavior of water/oil/surfactant systems using dissipative particle dynamics simulation, Advances in Colloid and Interface Science 309 (2022) 102774.

[20] M.L. Greenfield, Molecular modelling and simulation of asphaltenes and bituminous materials, International Journal of Pavement Engineering 12(4) (2011) 325-341.

[21] Z. Chen, J. Pei, R. Li, F. Xiao, Performance characteristics of asphalt materials based on molecular dynamics simulation – A review, Construction and Building Materials 189 (2018) 695-710.

[22] P. Wang, Z. Dong, Y. Tan, Z. Liu, Investigating the Interactions of the Saturate, Aromatic, Resin, and Asphaltene Four Fractions in Asphalt Binders by Molecular

1263 Simulations, Energy & Fuels 29(1) (2015) 112-121.
1264 [23] M. Su, J. Zhou, J. Lu, W. Chen, H. Zhang, Using molecular dynamics and
1265 experiments to investigate the morphology and micro-structure of SBS modified
1266 asphalt binder, Materials Today Communications 30 (2022) 103082.
1267 [24] Y. Li, H. Zhang, Z. Wu, B. Sun, Influencing Factors and Evaluation of the Self-
1268 Healing Behavior of Asphalt Binder Using Molecular Dynamics Simulation
1269 Method, Molecules 28(6) (2023) 2860.
1270 [25] L. He, Y. Zheng, A. Alexiadis, A. Cannone Falchetto, G. Li, J. Valentin, W. Van
1271 den bergh, Y. Emmanuilovich Vasiliev, K.J. Kowalski, J. Grenfell, Research on the
1272 self-healing behavior of asphalt mixed with healing agents based on molecular
1273 dynamics method, Construction and Building Materials 295 (2021) 123430.
1274 [26] H. Xiang, Z. He, H. Tang, M. Hu, Healing behavior of thermo-oxygen aged asphalt
1275 based on molecular dynamics simulations, Construction and Building Materials
1276 349 (2022) 128740.
1277 [27] H. Yao, Q. Dai, Z. You, Chemo-physical analysis and molecular dynamics (MD)
1278 simulation of moisture susceptibility of nano hydrated lime modified asphalt
1279 mixtures, Construction and Building Materials 101 (2015) 536-547.
1280 [28] S. Ren, X. Liu, P. Lin, Y. Gao, S. Erkens, Molecular dynamics simulation on bulk
1281 bitumen systems and its potential connections to macroscale performance: Review
1282 and discussion, Fuel 328 (2022) 125382.
1283 [29] H.-n. Wang, H.-y. Ding, P.-n. Feng, L.-l. Shao, X. Qu, Z.-p. You, Advances on

molecular simulation technique in asphalt mixture, Journal of Traffic and Transportation Engineering 20(2) (2020) 1-14.

[30] S. Ren, X. Liu, P. Lin, Y. Gao, S. Erkens, Review on the diffusive and interfacial performance of bituminous materials: From a perspective of molecular dynamics simulation, Journal of Molecular Liquids 366 (2022) 120363.

[31] H. Yao, J. Liu, M. Xu, J. Ji, Q. Dai, Z. You, Discussion on molecular dynamics (MD) simulations of the asphalt materials, Advances in Colloid and Interface Science 299 (2022) 102565.

[32] J. Xu, B. Ma, W. Mao, W. Si, X. Wang, Review of interfacial adhesion between asphalt and aggregate based on molecular dynamics, Construction and Building Materials 362 (2023) 129642.

[33] J.S. Hansen, C. Lemarchand, E. Nielsenn, J.C. Dyre, T. Schroder, Four-component united-atom model of bitumen, Journal of Chemical Physics 138(9) (2013).

[34] C.A. Lemarchand, T.B. Schroder, J.C. Dyre, J.S. Hansen, Cooee bitumen: Chemical aging, Journal of Chemical Physics 139(12) (2013).

[35] D.D. Li, M.L. Greenfield, Chemical compositions of improved model asphalt systems for molecular simulations, Fuel 115 (2014) 347-356.

[36] D.D. Li, M.L. Greenfield, Viscosity, relaxation time, and dynamics within a model asphalt of larger molecules, Journal of Chemical Physics 140(3) (2014) 034507.

[37] X. Yao, C. Li, T. Xu, Multi-scale studies on interfacial system compatibility between asphalt and SBS modifier using molecular dynamics simulations and

1305 experimental methods, Construction and Building Materials 346 (2022) 128502.
1306 [38] M. Su, C. Si, Z. Zhang, H. Zhang, Molecular dynamics study on influence of Nano-
1307 ZnO/SBS on physical properties and molecular structure of asphalt binder, Fuel
1308 263 (2020) 116777.
1309 [39] G. Li, Y. Tan, Y. Fu, P. Liu, C. Fu, M. Oeser, Density, zero shear viscosity and
1310 microstructure analysis of asphalt binder using molecular dynamics simulation,
1311 Construction and Building Materials 345 (2022) 128332.
1312 [40] G. Li, Y. Tan, The construction and application of asphalt molecular model based
1313 on the quantum chemistry calculation, Fuel 308 (2022) 122037.
1314 [41] G. Li, Z. Chen, Y. Tan, X. Cong, Y. Dong, S. Xiao, Experimental and molecular
1315 dynamics simulation of hard asphalt microstructure, Construction and Building
1316 Materials 377 (2023) 131025.
1317 [42] Y. Yang, Y. Wang, J. Cao, Z. Xu, Y. Li, Y. Liu, Reactive molecular dynamic
1318 investigation of the oxidative aging impact on asphalt, Construction and Building
1319 Materials 279 (2021) 121298.
1320 [43] D. Hu, X. Gu, B. Cui, J. Pei, Q. Zhang, Modeling the Oxidative Aging Kinetics
1321 and Pathways of Asphalt: A ReaxFF Molecular Dynamics Study, Energy & Fuels
1322 34(3) (2020) 3601-3613.
1323 [44] M. Gong, B. Jiao, Thermodynamic properties analysis of warm-mix recycled
1324 asphalt binders using molecular dynamics simulation, Road Materials and
1325 Pavement Design (2023) 2199883.

[45] S. Ren, X. Liu, P. Lin, Y. Gao, S. Erkens, Insight into the compatibility behaviors between various rejuvenators and aged bitumen: Molecular dynamics simulation and experimental validation, Materials & Design 223 (2022) 111141.

[46] X. Qu, Q. Liu, M. Guo, D. Wang, M. Oeser, Study on the effect of aging on physical properties of asphalt binder from a microscale perspective, Construction and Building Materials 187 (2018) 718-729.

[47] G. Xu, H. Wang, Molecular dynamics study of oxidative aging effect on asphalt binder properties, Fuel 188 (2017) 1-10.

[48] L. Luo, L. Chu, T.F. Fwa, Molecular dynamics analysis of oxidative aging effects on thermodynamic and interfacial bonding properties of asphalt mixtures, Construction and Building Materials 269 (2021) 121299.

[49] D. Hu, X. Gu, F. Yang, Z. Zhou, W. Bo, B. Cui, J. Pei, Atomic mechanisms of separation failure at the asphalt–aggregate interface and its dependence on aging and rejuvenation: Insights from molecular dynamics simulations and DFT calculations, Applied Surface Science 598 (2022) 153775.

[50] L. Guo, L. Pan, Z. Lv, Y. Chen, Cohesive zone model of asphalt-aggregate interface under compression and shear, Molecular Simulation 49(7) (2023) 643-654.

[51] S. Duan, J. Hu, T. Ma, X. Quan, Anti-icing mechanism of an environmentally sustainable tenebrio molitor antifreeze protein modified asphalt binder via molecular dynamics simulations, Construction and Building Materials 360 (2022) 129580.

1347 [52] H. Yao, Q. Dai, Z. You, Molecular dynamics simulation of physicochemical
1348 properties of the asphalt model, Fuel 164 (2016) 83-93.
1349 [53] X. Zhou, X. Zhang, S. Xu, S. Wu, Q. Liu, Z. Fan, Evaluation of thermo-mechanical
1350 properties of graphene/carbon-nanotubes modified asphalt with molecular
1351 simulation, Molecular Simulation 43(4) (2017) 312-319.
1352 [54] B. Sun, X. Zhou, Diffusion and Rheological Properties of Asphalt Modified by
1353 Bio-Oil Regenerant Derived from Waste Wood, Journal of Materials in Civil
1354 Engineering 30(2) (2018) 04017274.
1355 [55] L. Wang, Z. Li, Molecular Dynamics Simulation and Experimental Analysis of the
1356 Effect of Ultrasonic Disposal on the Compatibility of NanoAsphalt, Coatings 12(4)
1357 (2022).
1358 [56] C.M. Fedo, I.O. McGlynn, H.Y. McSween, Grain size and hydrodynamic sorting
1359 controls on the composition of basaltic sediments: Implications for interpreting
1360 martian soils, Earth and Planetary Science Letters 423 (2015) 67-77.
1361 [57] X. Chen, Y. Zhang, H. Huo, Z. Wu, Study of high tensile strength of natural
1362 continuous basalt fibers, Journal of Natural Fibers 17(2) (2018) 214-222.
1363 [58] N. Zaini, F. van der Meer, F. van Ruitenbeek, B. de Smeth, F. Amri, C. Lievens,
1364 An Alternative Quality Control Technique for Mineral Chemistry Analysis of
1365 Portland Cement-Grade Limestone Using Shortwave Infrared Spectroscopy,
1366 Remote Sensing 8(11) (2016) 950.
1367 [59] Z. Fan, J. Lin, J. Xu, B. Hong, P. Liu, D. Wang, M. Oeser, Molecular Insights into

1368 the Adsorption Configuration of Bitumen Colloidal on Aggregate Surface, Journal
1369 of Materials in Civil Engineering 34(4) (2022) 04022033.
1370 [60] Z. Fan, J. Lin, Z. Chen, P. Liu, D. Wang, M. Oeser, Multiscale understanding of
1371 interfacial behavior between bitumen and aggregate: From the aggregate
1372 mineralogical genome aspect, Construction and Building Materials 271 (2021)
1373 121607.
1374 [61] Y. Tang, Z. Fu, F. Ma, P. Zhao, Y. Hou, X. Jiang, C. Peng, Effect of water molecular
1375 behavior on adhesion properties of asphalt-aggregate interface, Construction and
1376 Building Materials 402 (2023) 133028.
1377 [62] G. Sun, Z. Niu, J. Zhang, X. Tan, Y. Jing, Z. Chen, Impacts of asphalt and mineral
1378 types on interfacial behaviors: A molecular dynamics study, Case Studies in
1379 Construction Materials 17 (2022) e01581.
1380 [63] Z. Dong, Z. Liu, P. Wang, X. Gong, Nanostructure characterization of asphalt-
1381 aggregate interface through molecular dynamics simulation and atomic force
1382 microscopy, Fuel 189 (2017) 155-163.
1383 [64] Z. Liu, H. Wang, X. Gong, P. Cui, H. Wei, Stiffening and Toughening of Asphalt
1384 Mastic Induced by Bitumen–Mineral Selective Molecular Adsorption and
1385 Nanostructural Reconstruction, Sustainability 15(5) (2023) 4398.
1386 [65] J. Du, Y. Jin, S. Hou, R. Jin, Q. Wang, Effect of component characteristics on
1387 mechanical properties of asphalt: A molecular dynamics study, Case Studies in
1388 Construction Materials 18 (2023) e02007.

[66] G. Xu, H. Wang, Molecular dynamics study of interfacial mechanical behavior between asphalt binder and mineral aggregate, Construction and Building Materials 121 (2016) 246-254.

[67] Z. Du, X. Zhu, F. Li, S. Zhou, Z. Dai, Failure of the Asphalt-Aggregate Interface under Tensile Stress: Insight from Molecular Dynamics, Journal of Materials in Civil Engineering 33(3) (2021) 04021008.

[68] M. Zhai, J. Li, R. Wang, J. Yue, X. Wang, Revealing Mechanisms of Aging and Moisture on Thermodynamic Properties and Failure Patterns of Asphalt-Aggregate Interface from the Molecular Scale, Journal of Materials in Civil Engineering 35(3) (2023) 04022486.

[69] P. Chen, X. Luo, Y. Gao, Y. Zhang, Modeling percentages of cohesive and adhesive debonding in bitumen-aggregate interfaces using molecular dynamics approaches, Applied Surface Science 571 (2022) 151318.

[70] H. Wang, E. Lin, G. Xu, Molecular dynamics simulation of asphalt-aggregate interface adhesion strength with moisture effect, International Journal of Pavement Engineering 18(5) (2017) 414-423.

[71] B. Cui, H. Wang, Molecular modeling of asphalt-aggregate debonding potential under moisture environment and interface defect, Applied Surface Science 606 (2022) 154858.

[72] Q. Wang, R. Yu, G. Fu, X. Chen, L. Cai, Y. Xiao, X. Zhang, X. Zhu, The short-term aging effect on the interface and surface wetting behavior of modified asphalt

1410 mixtures, Materials Research Express 9(8) (2022) 085102.
1411 [73] H. Yao, Q. Dai, Z. You, J. Zhang, S. Lv, X. Xiao, Evaluation of contact angle
1412 between asphalt binders and aggregates using Molecular Dynamics (MD) method,
1413 Construction and Building Materials 212 (2019) 727-736.
1414 [74] P. Cong, Z. Chen, W. Ge, Influence of moisture on the migration of asphalt
1415 components and the adhesion between asphalt binder and aggregate, Construction
1416 and Building Materials 385 (2023) 131513.
1417 [75] D. Niu, Z. Zhang, J. Meng, Z. Yang, R. Jing, X. Liu, P. Lin, Y. Sheng, Surface
1418 Modification of Steel Slag Aggregate for Engineering Application in Asphalt
1419 Mixture, Buildings 13(1) (2022) 16.
1420 [76] Z. Du, X. Zhu, Surface-Roughness-Induced Control of the Interfacial Failure Mode
1421 and Bonding Strength: Atomistic Case Study in an Asphalt-Aggregate System,
1422 Journal of Materials in Civil Engineering 34(12) (2022) 14.
1423 [77] Z. Long, L. You, X. Tang, W. Ma, Y. Ding, F. Xu, Analysis of interfacial adhesion
1424 properties of nano-silica modified asphalt mixtures using molecular dynamics
1425 simulation, Construction and Building Materials 255 (2020) 119354.
1426 [78] M. Ahmadi, M. Clarke, Z. Chen, The effect of bitumen molecular fractions on
1427 diffusivity and rheology of bitumen under high-temperature conditions: Molecular
1428 dynamics (MD) simulation study, Canadian Journal of Chemical Engineering
1429 101(3) (2023) 1150-1161.
1430 [79] C. Zheng, C. Shan, J. Liu, T. Zhang, X. Yang, D. Lv, Microscopic adhesion

properties of asphalt–mineral aggregate interface in cold area based on molecular simulation technology, Construction and Building Materials 268 (2021) 121151.

[80] Y. Yang, X. Liang, X. Li, Investigation of clay-oil interfacial interactions in petroleum-contaminated soil: Effect of crude oil composition, Journal of Molecular Liquids 380 (2023) 121702.

[81] X. Ma, J. Wu, Q. Liu, W. Ren, M. Oeser, Molecular dynamics simulation of the bitumen-aggregate system and the effect of simulation details, Construction and Building Materials 285 (2021) 122886.

[82] W. Sun, H. Wang, Molecular dynamics simulation of nano-crack formation in asphalt binder with different SARA fractions, Molecular Simulation 48(9) (2022) 789-800.

[83] R. Zhai, P. Hao, Research on the impact of mineral type and bitumen ageing process on asphalt-mineral adhesion performance based on molecular dynamics simulation method, Road Materials and Pavement Design 22(9) (2021) 2000-2013.

[84] X. Zhou, G. Zhao, S. Tighe, M. Chen, S. Wu, S. Adhikari, Y. Gao, Quantitative comparison of surface and interface adhesive properties of fine aggregate asphalt mixtures composed of basalt, steel slag, and andesite, Construction and Building Materials 246 (2020) 118507.

[85] J. Liu, B. Yu, S. Wang, L. Li, J. Zhang, Use of tricalcium silicate to evaluate asphalt absorption on steel slag: Atomic simulation and micro-scale characterization, Measurement 177 (2021) 109224.

[86] R. Li, H. Du, Z. Fan, J. Pei, Molecular Dynamics Simulation to Investigate the Interaction of Asphaltene and Oxide in Aggregate, Advances in Materials Science and Engineering 2016 (2016).

[87] Y. Yang, J. Song, H. Sui, L. He, X. Li, Understanding the behaviors of toluene in asphaltenes, Journal of Molecular Liquids 348 (2022) 118016.

[88] M. Shishehbor, M.R. Pouranian, R. Imaninasab, Evaluating the adhesion properties of crude oil fractions on mineral aggregates at different temperatures through reactive molecular dynamics, Petroleum Science and Technology 36(24) (2018) 2084-2090.

[89] D. Hu, X. Gu, L. Lyu, J. Pei, B. Cui, Investigating the aging mechanism of asphaltene and its dependence on environmental factors through AIMD simulations and DFT calculations, Science of The Total Environment 795 (2021) 148897.

[90] W. Cao, E. Fini, A Molecular Dynamics Approach to the Impacts of Oxidative Aging on the Engineering Characteristics of Asphalt, Polymers 14 (2022) 2916.

[91] C. Bao, C. Zheng, Y. Xu, L. Nie, H. Luo, Microscopic analysis of the evolution of asphalt colloidal properties and rejuvenation behavior in aged asphalt, Journal of Cleaner Production 339 (2022) 130761.

[92] M. Deng, X. Cao, Z. Li, X. Li, X. Yang, B. Tang, Investigating properties and intermolecular interactions of sludge bio-oil modified asphalt, Journal of Molecular Liquids 360 (2022) 119415.

1473 [93] Z. Fu, Y. Tang, C. Peng, F. Ma, C. Li, Properties of polymer modified asphalt by
1474 polyphosphoric acid through molecular dynamics simulation and experimental
1475 analysis, Journal of Molecular Liquids 382 (2023) 121999.
1476 [94] L. Chu, L. Luo, T.F. Fwa, Effects of aggregate mineral surface anisotropy on
1477 asphalt-aggregate interfacial bonding using molecular dynamics (MD) simulation,
1478 Construction and Building Materials 225 (2019) 1-12.
1479 [95] G. Xu, H. Wang, Study of cohesion and adhesion properties of asphalt concrete
1480 with molecular dynamics simulation, Computational Materials Science 112 (2016)
1481 161-169.
1482 [96] W. Cui, W. Huang, Z. Xiao, J. Xie, B. Hu, X. Cai, K. Wu, The Effect of Moisture
1483 on the Adhesion Energy and Nanostructure of Asphalt-Aggregate Interface System
1484 Using Molecular Dynamics Simulation, Molecules 25(18) (2020).
1485 [97] Y.L. Yaphary, M. He, G. Lu, F. Zou, P. Liu, D.C.W. Tsang, Z. Leng, Experiment
1486 and multiscale molecular simulations on the Cu absorption by biochar-modified
1487 asphalt: An insight into removal capability and mechanism of heavy metals from
1488 stormwater runoff, Chemical Engineering Journal 462 (2023) 142205.
1489 [98] H. Zhang, J. Cao, H. Duan, H. Luo, X. Liu, Molecular dynamics insight into the
1490 adsorption and distribution of bitumen subfractions on Na-montmorillonite
1491 surface, Fuel 310 (2022) 122380.
1492 [99] F. Guo, J. Pei, G. Huang, J. Zhang, A. Cannone Falchetto, L. Korkiala-Tanttu,
1493 Investigation of the adhesion and debonding behaviors of rubber asphalt and

aggregates using molecular dynamics simulation, Construction and Building Materials 371 (2023) 130781.

[100] Y. Gao, Y. Zhang, F. Gu, T. Xu, H. Wang, Impact of minerals and water on bitumen-mineral adhesion and debonding behaviours using molecular dynamics simulations, Construction and Building Materials 171 (2018) 214-222.

[101] J. Li, Z. Wang, M. Jia, Comprehensive analysis on influences of aggregate, asphalt and moisture on interfacial adhesion of aggregate-asphalt system, Journal of Adhesion Science and Technology 35(6) (2021) 641-662.

[102] B. Xing, Y. Du, C. Fang, H. Sun, Y. Lyu, W. Fan, Particle morphology of mineral filler and its effects on the asphalt binder-filler interfacial interaction, Construction and Building Materials 321 (2022) 126292.

[103] P. Feng, H. Wang, H. Ding, J. Xiao, M. Hassan, Effects of surface texture and its mineral composition on interfacial behavior between asphalt binder and coarse aggregate, Construction and Building Materials 262 (2020) 120869.

[104] Y. Gong, J. Xu, E.-h. Yan, Intrinsic temperature and moisture sensitive adhesion characters of asphalt-aggregate interface based on molecular dynamics simulations, Construction and Building Materials 292 (2021) 123462.

[105] G. Huang, J. Zhang, Z. Wang, F. Guo, Y. Li, L. Wang, Y. He, Z. Xu, X. Huang, Evaluation of asphalt-aggregate adhesive property and its correlation with the interaction behavior, Construction and Building Materials 374 (2023) 130909.

[106] L. Zhang, N. Long, Y. Liu, L. Wang, Cross-scale study on the influence of

moisture-temperature coupling conditions on adhesive properties of rubberized asphalt and steel slag, Construction and Building Materials 332 (2022) 127401.

[107] Z. Du, X. Zhu, Y. Zhang, Diffusive Dynamics and Structural Organization of Moisture in Asphaltic Materials Based on Molecular Dynamics Simulation, Journal of Materials in Civil Engineering 33(1) (2021) 04020403.

[108] L. Luo, L. Chu, T.F. Fwa, Molecular dynamics analysis of moisture effect on asphalt-aggregate adhesion considering anisotropic mineral surfaces, Applied Surface Science 527 (2020) 146830.

[109] W. Sun, H. Wang, Moisture effect on nanostructure and adhesion energy of asphalt on aggregate surface: A molecular dynamics study, Applied Surface Science 510 (2020).

[110] W. Cui, W. Huang, B. Hu, J. Xie, Z. Xiao, X. Cai, K. Wu, Investigation of the Effects of Adsorbed Water on Adhesion Energy and Nanostructure of Asphalt and Aggregate Surfaces Based on Molecular Dynamics Simulation, Polymers 12(10) (2020) 2339.

[111] H. Yao, J. Liu, Y. Wang, X. li, J. Zeng, J. Li, J. Ji, Q. Dai, Z. You, Mechanism exploration of the foamed asphalt binder using the Molecular Dynamics (MD) method, Journal of Cleaner Production 374 (2022) 134015.

[112] J.Y. Mane, S.R. Stoyanov, Molecular dynamics investigation of the asphaltene-kaolinite interactions in water, toluene, and water-toluene mixtures, Physical Chemistry Chemical Physics 25(7) (2023) 5638-5647.

[113] C. Peng, L. Lu, Z. You, F. Xu, L. You, M. Miljković, C. Guo, S. Huang, H. Ma, Y. Hu, Y. Liu, J. Dai, J. Zhu, H. Bi, Influence of silane-hydrolysate coupling agents on bitumen–aggregate interfacial adhesion: An exploration from molecular dynamics simulation, International Journal of Adhesion and Adhesives 112 (2022) 102993.

[114] Y. Cheng, H. Wang, L. Li, J. Liang, A Multi-scale Study of SBS Modified Asphalt-Aggregate Adhesion Under Moisture Damage, Arabian Journal for Science and Engineering (2023).

[115] B. Cui, H. Wang, Molecular interaction of Asphalt-Aggregate interface modified by silane coupling agents at dry and wet conditions, Applied Surface Science 572 (2022) 151365.

[116] T. Yu, H. Zhang, J. Sun, D. Chen, H. Wang, Y. Feng, Influence of freezing and thawing on drainage behaviour for porous asphalt pavement based on molecular dynamics simulation, International Journal of Pavement Engineering (2021) 1-12.

[117] E. Lee, D.H. Kim, Simple fabrication of asphalt-based superhydrophobic surface with controllable wetting transition from Cassie-Baxter to Wenzel wetting state, Colloids and Surfaces A: Physicochemical and Engineering Aspects 625 (2021) 126927.

[118] X. Zhou, Q. Huang, S. Xu, Multi-scale analysis of moisture diffusion and distribution in different types of asphalt mixtures, International Journal of

Pavement Engineering 23(2) (2022) 187-196.

[119] X. Zhou, T.B. Moghaddam, M. Chen, S. Wu, S. Adhikari, F. Wang, Z. Fan, Nano-scale analysis of moisture diffusion in asphalt-aggregate interface using molecular simulations, Construction and Building Materials 285 (2021) 122962.

[120] Q. Guo, L. Li, Y. Jiao, M. Guo, W. Wang, W. Yu, W. He, Experimental measurements of the moisture diffusion and strength damage mechanism of dense asphalt mixtures, International Journal of Pavement Engineering 24(1) (2023) 2198772.

[121] Z. Long, L. You, F. Xu, X. Tang, Y. Ding, A. Khanal, Y. Miao, Nanomechanical-atomistic insights on interface interactions in asphalt mixtures with various chloride ion erosion statuses, Journal of Colloid and Interface Science 628(Pt A) (2022) 891-909.

[122] Z. Long, X. Tang, Y. Ding, M. Miljković, A. Khanal, W. Ma, L. You, F. Xu, Influence of sea salt on the interfacial adhesion of bitumen–aggregate systems by molecular dynamics simulation, Construction and Building Materials 336 (2022) 127471.

[123] Z. Long, N. Guo, X. Tang, Y. Ding, L. You, F. Xu, Microstructural evolution of asphalt induced by chloride salt erosion, Construction and Building Materials 343 (2022) 128056.

[124] Z. Long, L. You, N. Guo, F. Xu, X. Tang, Y. Ding, Influence of mineral composition on nano-interfacial adhesion of asphalt mixtures exposed to chloride

1578 salt erosion, Construction and Building Materials 367 (2023) 130213.
1579 [125] Y. Meng, J. Lai, S. Mo, G. Fang, S. Deng, X. Wei, F. Yang, Investigating the
1580 deterioration mechanism of adhesion between asphalt and aggregate interface
1581 under acid rain erosion, Applied Surface Science 639 (2023) 158171.
1582 [126] C. Li, W. Qin, Z. Fu, J. Dai, F. Ma, Comparative evaluation on decay process of
1583 asphalt-aggregate interfaces under solution erosion, Construction and Building
1584 Materials 400 (2023) 132698.
1585 [127] C. Li, F. Ma, Z. Fu, J. Dai, Y. Wen, K. Shi, Investigation of the solution effects
1586 on asphalt binder and mastic through molecular dynamics simulations,
1587 Construction and Building Materials 345 (2022) 128314.
1588 [128] X. Chen, D. Ren, G. Tian, J. Xu, R. Ali, C. Ai, Investigation on moisture damage
1589 resistance of asphalt pavement in salt and acid erosion environments based on
1590 Multi-scale analysis, Construction and Building Materials 366 (2023) 130177.
1591 [129] Y.L. Yaphary, Z. Leng, H. Wang, S. Ren, G. Lu, Characterization of nanoscale
1592 cracking at the interface between virgin and aged asphalt binders based on
1593 molecular dynamics simulations, Construction and Building Materials 335 (2022)
1594 127475.
1595 [130] W. Cui, K. Huo, S. Sugiyama, Y. Liang, Y. Masuda, M. Morimoto, T. Matsuoka,
1596 E.S. Boek, Y. Kaito, K. Nakagawa, D. Ito, Microstructural evolution of bitumen
1597 during the glass transition: An application of digital oil, Fuel 335 (2023) 127048.
1598 [131] M. Li, S. Li, C. Zhu, N. Li, H. Wang, N.I. Md. Yusoff, Effect of Iron Oxide on

Self-Healing and Thermal Characteristics of Asphalt Based on Molecular Dynamics Simulation Perspective, Advances in Materials Science and Engineering 2022 (2022) 1-14.

[132] Y. Tang, Z. Fu, J. Liu, F. Ma, C. Peng, C. Li, X. Chang, P. Zhao, Molecular dynamics simulation and experimental analysis on fluidity improvement of liquid rubber modified asphalt binder, Construction and Building Materials 402 (2023) 133027.

[133] K. Wei, Y. Su, X. Cao, T. Jiang, M. Deng, Y. Wu, Molecular Dynamics Simulation of Interaction between Polymer Modifier and Asphalt, Journal of Testing and Evaluation 50(4) (2022) 2175-2189.

[134] K. Hu, C. Yu, Y. Chen, W. Li, D. Wang, W. Zhang, Multiscale mechanisms of asphalt performance enhancement by crumbed waste tire rubber: insight from molecular dynamics simulation, Journal of Molecular Modeling 27(6) (2021).

[135] L. Wang, Y. Liu, L. Zhang, A Multiscale Study of Moisture Influence on the Crumb Rubber Asphalt Mixture Interface, Applied Sciences 12(14) (2022) 6940.

[136] B. Jiao, B. Pan, T. Che, Evaluating impacts of desulfurization and depolymerization on thermodynamics properties of crumb rubber modified asphalt through molecular dynamics simulation, Construction and Building Materials 323 (2022) 126360.

[137] F. Guo, J. Zhang, J. Pei, B. Zhou, A.C. Falchetto, Z. Hu, Investigating the interaction behavior between asphalt binder and rubber in rubber asphalt by

molecular dynamics simulation, Construction and Building Materials 252 (2020) 118956.

[138] A.S. Mohamed, W. Wang, H. Weng, Y. Fang, F. Xiao, Impacts of colloidal and interfacial interactions on bonding strength of rubberized RAP asphalt binder, Construction and Building Materials 349 (2022) 128768.

[139] Y. Tang, Z. Fu, F. Ma, J. Liu, Q. Sun, C. Li, Carbon nanotubes for improving rheological and chemical properties of styrene–butadiene–styrene modified asphalt binder, International Journal of Pavement Engineering 24(1) (2023) 2211212.

[140] G. Li, Z. Gu, Y. Tan, C. Xing, J. Zhang, C. Zhang, Research on the phase structure of Styrene-Butadiene-Styrene modified asphalt based on molecular dynamics, Construction and Building Materials 326 (2022) 126933.

[141] F. Guo, J. Pei, J. Zhang, R. Li, P. Liu, D. Wang, Study on Adhesion Property and Moisture Effect between SBS Modified Asphalt Binder and Aggregate Using Molecular Dynamics Simulation, materials 15(19) (2022) 6912.

[142] H. Dan, Z. Zou, Z. Zhang, J. Tan, Effects of aggregate type and SBS copolymer on the interfacial heat transport ability of asphalt mixture using molecular dynamics simulation, Construction and Building Materials 250 (2020) 118922.

[143] X. Zhou, S. Wu, G. Liu, P. Pan, Molecular simulations and experimental evaluation on the curing of epoxy bitumen, Materials and Structures 49(1-2) (2016) 241-247.

[144] R. Yu, Q. Wang, W. Wang, Y. Xiao, Z. Wang, X. Zhou, X. Zhang, X. Zhu, C. Fang, Polyurethane/graphene oxide nanocomposite and its modified asphalt binder: Preparation, properties and molecular dynamics simulation, Materials & Design 209 (2021) 109994.

[145] S. Zhao, H. Zhang, Y. Feng, Y. Hang, Effect of diffusion on interfacial properties of polyurethane-modified asphalt–aggregate using molecular dynamic simulation, Reviews on Advanced Materials Science 61(1) (2022) 778-794.

[146] P. Lu, Y. Ma, K. Ye, S. Huang, Analysis of high-temperature performance of polymer-modified asphalts through molecular dynamics simulations and experiments, Construction and Building Materials 350 (2022) 128903.

[147] W. Cui, W. Huang, H.M.Z. Hassan, X. Cai, K. Wu, Study on the interfacial contact behavior of carbon nanotubes and asphalt binders and adhesion energy of modified asphalt on aggregate surface by using molecular dynamics simulation, Construction and Building Materials 316 (2022) 125849.

[148] S. Wang, X. Chen, X. Zhang, F. Liu, Y. Gao, F. Li, Effect of ionic emulsifiers on the properties of emulsified asphalts: An experimental and simulation study, Construction and Building Materials 347 (2022) 13.

[149] Q. Yang, C. Yu, Multiscale Enhancement Mechanism of Carbon Nanotube-Modified Asphalt at High Temperature by Oxidative Aging: A Molecular Dynamics Simulation Investigation, Energy & Fuels 36(24) (2022) 15279-15296.

[150] L. Wang, L. Zhang, Y. Liu, Molecular Dynamics Study on the Effect of Mineral

Composition on the Interface Interaction between Rubberized Asphalt and Aggregate, Journal of Materials in Civil Engineering 34(4) (2022) 04022032.

[151] X. Yao, C. Li, T. Xu, Interfacial adhesive behaviors between SBS modified bitumen and aggregate using molecular dynamics simulation, Surfaces and Interfaces 33 (2022) 102245.

[152] G. Xu, Y.S. Yao, M. Wu, Y.L. Zhao, Molecular simulation and experimental analysis on co-aging behaviors of SBS modifier and asphalt in SBS-modified asphalt, Molecular Simulation 49(7) (2023) 629-642.

[153] B. Cui, H. Wang, Oxidative aging mechanism of asphalt binder using experiment-derived average molecular model and ReaxFF molecular dynamics simulation, Fuel 345 (2023) 128192.

[154] Y. Ding, M. Deng, X. Cao, M. Yu, B. Tang, Investigation of mixing effect and molecular aggregation between virgin and aged asphalt, Construction and Building Materials 221 (2019) 301-307.

[155] B. Cui, X. Gu, H. Wang, D. Hu, Numerical and experimental evaluation of adhesion properties of asphalt-aggregate interfaces using molecular dynamics simulation and atomic force microscopy, Road Materials and Pavement Design 23(7) (2022) 1564-1584.

[156] T. Yu, H. Zhang, Y. Wang, Interaction of asphalt and water between porous asphalt pavement voids with different aging stage and its significance to drainage, Construction and Building Materials 252 (2020) 119085.

[157] C. Peng, H. Yang, Z. You, H. Ma, F. Xu, L. You, A. Diab, L. Lu, Y. Hu, Y. Liu, J. Dai, Z. Li, Investigation of Adhesion Performance of Wax Based Warm Mix Asphalt with Molecular Dynamics Simulation, materials 15(17) (2022) 5930.

[158] T. Zhen, X. Kang, J. Liu, B. Zhang, W. Si, T. Ling, Multiscale Evaluation of Asphalt Aging Behaviour: A Review, Sustainability 15(4) (2023) 2953.

[159] L. Luo, P. Liu, S. Leischner, M. Oeser, Atomic insight into the nano-cracking behaviour of bitumen: considering oxidative aging effects, Road Materials and Pavement Design (2023) 1-16.

[160] Y. Gao, Y. Zhang, Y. Yang, J. Zhang, F. Gu, Molecular dynamics investigation of interfacial adhesion between oxidised bitumen and mineral surfaces, Applied Surface Science 479 (2019) 449-462.

[161] H. Zhang, Y. Wang, T. Yu, Z. Liu, Microstructural characteristics of differently aged asphalt samples based on atomic force microscopy (AFM), Construction and Building Materials 255 (2020) 119388.

[162] Y. Meng, Z. Wang, J. Lei, Y. Liao, X. Zhao, Y. Qin, G. Fang, C. Zhang, Study on aging resistance and micro characteristics of bio-asphalt/TLA composite modified asphalt binder, Construction and Building Materials 359 (2022) 129566.

[163] Z. Fu, Y. Tang, F. Ma, Y. Wang, K. Shi, J. Dai, Y. Hou, J. Li, Rheological properties of asphalt binder modified by nano-TiO2/ZnO and basalt fiber, Construction and Building Materials 320 (2022) 126323.

[164] J. Wang, Q. Li, Y. Lu, S. Luo, Effect of Waste-Oil regenerant on diffusion and

fusion behaviors of asphalt recycling using molecular dynamics simulation, Construction and Building Materials 343 (2022) 128043.

[165] S. Gulzar, A. Fried, J. Preciado, C. Castorena, S. Underwood, J. Habbouche, I. Boz, Towards sustainable roads: A State-of-the-art review on the use of recycling agents in recycled asphalt mixtures, Journal of Cleaner Production 406 (2023) 136994.

[166] Y. Tan, J. Xie, J. Song, J. Xu, X. Li, Interfacial interaction behavior of recycled asphalt pavement: Molecular dynamics simulation, Colloids and Surfaces A: Physicochemical and Engineering Aspects 676 (2023) 132194.

[167] Y. Ding, D. Li, Y. Wang, W. Wei, Prediction of the Rejuvenator Diffusion Coefficient in Aged Asphalt Based on Free Volume Theory, ACS Sustainable Chemistry & Engineering 11(1) (2022) 407-415.

[168] N. Xu, H. Wang, H. Wang, M. Kazemi, E. Fini, Research progress on resource utilization of waste cooking oil in asphalt materials: A state-of-the-art review, Journal of Cleaner Production 385 (2023) 135427.

[169] K. Shi, Z. Fu, J.Y. Liu, R.M. Song, F. Ma, J.S. Dai, C. Li, Y.L. Wen, Multiscale investigation of waste soybean oil rejuvenated asphalt binder utilising experimental methodologies and molecular dynamics simulations, International Journal of Pavement Engineering 24(1) (2023) 2181961.

[170] X. Zhang, Y. Ning, X. Zhou, X. Xu, X. Chen, Quantifying the rejuvenation effects of soybean-oil on aged asphalt-binder using molecular dynamics simulations,

1725 Journal of Cleaner Production 317 (2021) 128375.
1726 [171] K. Shi, Z. Fu, R.-m. Song, F.-l. Liu, F. Ma, J.-s. Dai, Waste chicken fat oil as a
1727 biomass regenerator to restore the performance of aged asphalt: rheological
1728 properties and regeneration mechanism, Road Materials and Pavement Design
1729 (2021) 1-25.
1730 [172] N. Xu, H. Wang, Y. Chen, N. Hossiney, Z. Ma, H. Wang, Insight into the effects
1731 of waste vegetable oil on self-healing behavior of bitumen binder, Construction
1732 and Building Materials 363 (2023) 129888.
1733 [173] S. Yan, C. Zhou, J. Zhang, G. Li, Molecular dynamics simulation on the
1734 rejuvenation effects of waste cooking oil on aged asphalt binder, Journal of Traffic
1735 and Transportation Engineering (English Edition) 9(5) (2022) 795-807.
1736 [174] H. Li, Q. Zhao, Z. Feng, F. Zhang, X. Zou, Recycling waste engine oil as a
1737 viscosity reducer for asphalt rubber: an insight from molecular dynamics
1738 simulations and laboratory tests, Environmental Science and Pollution Research
1739 (2022) 15.
1740 [175] W. Cao, Exploring the deagglomerating behaviors of selected additives on
1741 oxidized asphaltenes using the steered molecular dynamics approach, Journal of
1742 Molecular Liquids 375 (2023) 121327.
1743 [176] C. Bao, Y. Xu, C. Zheng, L. Nie, X. Yang, Rejuvenation effect evaluation and
1744 mechanism analysis of rejuvenators on aged asphalt using molecular simulation,
1745 Materials and Structures 55(2) (2022).

[177] K. Shi, F. Ma, J. Liu, Z. Fu, R. Song, D. Yuan, C. Li, Rejuvenation effect of aged SBS-modified asphalt utilizing molecule analysis, Journal of Cleaner Production 405 (2023) 136964.

[178] K. Shi, F. Ma, J. Liu, R.-m. Song, Z. Fu, J.-s. Dai, C. Li, Y.-l. Wen, Development of a new rejuvenator for aged SBS modified asphalt binder, Journal of Cleaner Production 380 (2022) 134986.

[179] K. Shi, Z. Fu, J. Liu, R. Song, F. Ma, J. Dai, C. Li, Y. Wen, Multiscale investigation of waste soybean oil rejuvenated asphalt binder utilising experimental methodologies and molecular dynamics simulations, International Journal of Pavement Engineering 24(1) (2023) 2181961.

[180] S. Yan, C. Zhou, J. Ouyang, Rejuvenation effect of waste cooking oil on the adhesion characteristics of aged asphalt to aggregates, Construction and Building Materials 327 (2022) 126907.

[181] X. Zheng, W. Xu, W. Ji, K. Cao, Study on the Wetting and Permeation Properties of Bio-Oil as Bitumen Rejuvenator, International Journal of Molecular Sciences 24(7) (2023) 6512.

[182] B. Cui, X. Gu, D. Hu, Q. Dong, A multiphysics evaluation of the rejuvenator effects on aged asphalt using molecular dynamics simulations, Journal of Cleaner Production 259 (2020) 120629.

[183] Q. Li, J. Wang, Y. Lu, X. Zhou, Y. Hu, J. Sun, G. Fu, Effect of dynamic water pressure on the adhesion behavior of recycled asphalt-aggregate interface by

molecular dynamics method, Construction and Building Materials 382 (2023) 131296.

[184] H. Yu, J. Ge, G. Qian, C. Zhang, W. Dai, P. Li, Evaluation on the rejuvenation and diffusion characteristics of waste cooking oil on aged SBS asphalt based on molecular dynamics method, Journal of Cleaner Production 406 (2023) 136998.